European and North Atlantic daily to MULtidecadal climate varaibility

EMULATE

EVK2-CT-2001-00161

Detailed project report: November 2002 to February 2006

Section 6: Detailed report, related to overall project duration

Co-ordinator: Prof. P.D. Jones (p.jones@uea.ac.uk)
Climatic Research Unit, University of East Anglia,
Norwich, NR4 7TJ, UK

EMULATE home page: http://www.cru.uea.ac.uk/projects/emulate/

THE EMULATE PARTNERS

1	UEA	University of East Anglia, UK
2	MetO	Meteorological Office, UK
3	UAUGS	Universitaet of Augsburg, Germany
4	CEA	CEA/DSM's Laboratoire des Sciences du Climat et de l'Environnement,
5	URV	University Rovira i Virgili, Tarragona, Spain
6	UBERN	University of Bern, Switzerland
7	SU	Stockholm University, Sweden
8	UGOT	University of Gothenburg, Sweden

CONTENTS

6.1 BACKGROUND

Studies of the influence of atmospheric circulation on surface climate variables are limited by data availability. The instrumental database is short and it is often difficult to discern if relationships are stationary or whether subtle changes are occurring. Europe has the longest of all instrumental climate records as the first instruments were developed here in the late 17th century. Although earlier projects have highlighted some of these records, others wait to be digitised and homogenised. EMULATE sought to extend continent-wide analyses back to the mid-19th century, providing 150 years of gridded daily pressure data for analysis. Homogeneity issues and digital availability, both of which were addressed, are the principal constraints on analyses of European/North Atlantic circulation patterns and their influence on surface climate variations. Many analyses begin in the mid-20th century when with some effort and care, they could begin in the mid-19th century.

EMULATE proposed to create daily gridded fields of mean-sea-level pressure (MSLP) over the extratropical North Atlantic and Europe (25ºN to 70ºN; 70ºW to 50ºE on a 5º by 5º grid spacing), 1850 to date. The database was used to develop time series of characteristic atmospheric circulation patterns for each season, sampled on sub-monthly time scales. The database was assessed for quality and the standard errors quantified for each time step and grid-point location. Variations and trends in these patterns, and associated temperature and precipitation patterns, were related to those evident in large-scale sea surface temperatures (SSTs) and other possible oceanic fluctuations. The work was undertaken with the aid of atmosphere only and coupled atmosphere and ocean models. Variations in the incidence of extremes of temperature and precipitation (including drought) across Europe were then related to fluctuations and trends in the atmospheric circulation patterns on daily to multi-decadal timescales and, for temperature, to SST and possible anthropogenic factors. With the new datasets and patterns, relationships can be investigated for much longer periods than available at the beginning of the project.

The longer daily MSLP record enables the assessment of the relative importance of anthropogenic factors to be more reliably determined. Relationships found (and their variability) were compared with results from the Hadley Centre atmosphere-only and coupled climate models. The project defined an array of extreme events over the last 150 years across Europe and determined the importance of atmospheric circulation changes, SST and external forcing factors. This enables the probable impacts of anthropogenic factors on extreme events to be determined over Europe.

Relationships also exist between regional-scale SST and atmospheric circulation patterns for the North Atlantic and the spatial and temporal scale of drought patterns in Europe. The temporal behaviour of such relationships was investigated, with special emphasis on studying possible anthropogenic influences. The Mediterranean region is particularly sensitive to droughts and any increased ability to predict future droughts would be of great benefit to these countries.

There is increasing concern that extreme climate (including weather timescale) events, which have major impacts on society and ecosystems, may be changing in frequency and character as a result of human influences on climate. The project defined these extreme events based on long daily temperature and precipitation series across Europe and attempted to determine the importance of atmospheric circulation changes. The project assessed the part human influences (directly or indirectly) may have played in changes in the frequency and severity of extreme events, additionally involving the use of climate model results.

6.2 SCIENTIFIC/TECHNOLOGICAL AND SOCIO-ECONOMIC OBJECTIVES

EMULATE had four principal objectives (Workpackages 1-4):

- Create daily gridded MSLP fields from 1850 for the region (25ºN to 70ºN; 70ºW to 50ºE on a 5º by 5º grid spacing).

- Derive a set of characteristic atmospheric circulation patterns, and study their variations and trends for each season (both the traditional ones as well as every 2-month 'season'.

- Relate variations and trends in atmospheric circulation and associated surface climate variability over Europe to sea surface temperature patterns, particularly from the North Atlantic.

- Relate variations and trends in atmospheric circulation patterns to prominent extremes in temperature and precipitation.

In addition to these, WP5 disseminated the project results via the web site and towards the end of the project gave details of papers in the scientific literature.

Fifteen measurable project objectives were identified:

- Digitize additional daily land station pressure data back to 1850.

- Integrate daily land station pressure data with marine pressure data from the I-COADS Data Set.

- Produce the daily gridded MSLP dataset (1850 to present) using the best method (which was Reduced Space Optimal Interpolation, RSOI).

- Define leading atmospheric circulation patterns from the gridded daily pressure dataset for each two-month and three-month seasons.

- Create a database of quantitative changes in pattern amplitudes of these circulation patterns since 1850.

- Assess the trends in these pattern amplitudes and in the incidence of their extremes.

- Characterise within-pattern variability.

- Assess the relationship between both SST and North Atlantic and European atmospheric circulation patterns and surface temperature and precipitation variability, through the seasonal cycle.

- Create a gridded database of drought severity (using the Palmer Drought Severity Index) across Europe.

- Assess the relative influence of external forcing factors (natural and anthropogenic) and internal climate variability and their seasonal differences, mainly through the use of climate models.

- Determine a selection of extreme climate indices for Europe and assessment of changes in these indices since 1850.

- Determine the significance of atmospheric circulation for the extreme indices.

- Ascertain whether extremes of climate had different characteristics in the late 20th century from those evident in the late 19th and early 20th centuries and determine the likely magnitude of human influences.

- Widely disseminate the project results (initially through the web site for the datasets and the specific deliverables) and later in the project through project reports, presentations at scientific meetings and scientific papers in the peer-reviewed literature.

6.3 APPLIED METHODOLOGY, SCIENTIFIC ACHIEVEMENTS AND MAIN DELIVERABLES

6.3.1 Work Package 1

Scientific achievements

The data set (referred to as EMSLP) was released to the EMULATE group in June, 2004 – completing Deliverables D2 and D3. All land station data (both 'uncorrected' and quality controlled station data series) used in the project were also made available on the EMULATE web site (part of Deliverable D4). A diagnostics report and a paper (Ansell *et al*., 2006) have also been produced; the former is also available from the web-site. EMSLP was developed from terrestrial and marine mean sea-level pressure (MSLP) data.

Terrestrial data sources
In all, 86 continental and island stations over the North-Atlantic European region (see Figure 1.1 for land station distribution) were selected for EMSLP. A detailed list of the individual station lengths is provided in Table 1.1.

Considerable material was digitised from individual hard copy records from Russian, United Kingdom (UK), French and Spanish daily weather records (DWRs), held in the UK National Meteorological Archives and Library. These were supplemented by scanned Algerian, French and US observations available from the NOAA library web site (http://docs.lib.noaa.gov/rescue/data_rescue_home.html). Old American 'Bulletin of International Meteorological observations' volumes also provided valuable records for Godthaab in Greenland and helped fill gaps in existing records. Data were also digitised from compilations made under the auspices of the UK Board of Trade, Royal Engineers and Army medical departments and from Ottoman Empire records also held in the UK National Meteorological Archives.

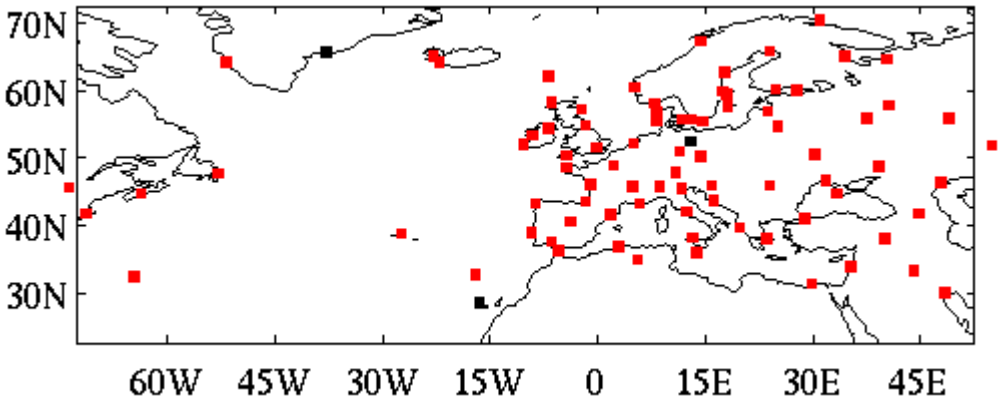

Figure 1.1: *Distribution of the 86 continental and island station in EMSLP. Red squares indicate stations whose records begin between 1850 and 1880. Black squares are for those stations whose records begin post 1880. 1850-1880 corresponds to the period when we have no Superfile (Jackson, 1986) data available.*

Station	first year	end year	lat.	long.	Station	first year	last year	lat.	long.
Aberdeen	1861	1995	57.16	-2.10	Alexandria	1876	1881	31.20	29.95
Algiers	1872	1881	36.76	3.10	Ammasalik	1894	1995	65.60	-37.63
Angra (de Heroismo)	1871	1878	38.66	-27.22	Archangel	1866	2000	64.55	40.53
Armagh	1850	2001	54.35	-6.65	Astrakhan	1850	2000	46.35	48.03
Athens	1850	1880	37.90	23.73	Baghdad	1869	1876	33.23	44.23
Barcelona	1850	2002	41.50	2.01	Beirut	1869	1876	33.82	35.48
Bergen	1868	2002	60.38	5.33	Bermuda	1852	1880	32.28	-64.50
Biarritz	1860	1880	43.46	-1.53	Biskra	1878	1881	34.80	5.73
Bodo	1868	1994	67.26	14.43	Brest	1861	1881	48.45	-4.16
Cadiz	1786	2002	37.46	-6.28	Corfu	1852	1880	39.61	19.91
De Bilt	1850	2001	52.10	5.18	Diyarbakir	1869	1876	37.88	40.18
Durham	1850	1881	54.76	-1.58	Fao (near Al Basrah)	1869	1876	29.98	48.50
Funchal	1871	1881	32.63	-16.90	Galway	1850	1880	53.28	-9.02
Gibraltar	1850	2002	36.10	-5.35	Godthaab	1850	1880	64.16	-51.75
Gothenburg	1860	2002	55.70	11.98	Halifax	1850	1875	44.63	-63.50
Hammerodde	1874	1995	55.30	14.78	Haparanda	1860	2002	65.82	24.13
Harnosand	1860	1995	62.61	17.93	Helsinki	1844	2001	60.17	24.95
Hohenpeissenberg	1850	2002	47.80	11.02	Jena	1850	2000	50.93	11.58
Kazan	1850	2000	55.78	49.13	Kem	1866	1880	64.95	34.65
Kiev	1850	1990	50.40	30.45	Kostroma	1850	1880	57.73	40.78
La Coruna	1865	2002	43.16	-8.50	Lesina (Split)	1869	1881	43.53	16.30
Lisbon	1869	1881	38.77	-9.13	London	1850	1881	51.46	0
Lugansk	1850	1880	48.60	39.30	Lund	1864	2001	55.70	13.20
Lyon	1869	1881	45.72	4.95	Madrid	1853	1880	40.45	-3.71
Malta	1852	1880	35.83	14.00	Milan	1763	1998	45.61	8.73
Montreal	1850	1873	45.53	-73.60	Moscow	1850	2000	55.76	37.66
Nikolayev	1850	1880	46.58	31.95	Nordby	1874	2002	55.43	8.40
Oksoyfyr	1870	2002	58.07	8.05	Orenburg	1850	1876	51.75	55.10
Padua	1766	1997	45.40	11.85	Palermo	1851	1880	38.13	13.33
Paris	1851	1880	48.81	2.33	Plymouth	1861	1881	50.35	-4.15
Potsdam	1893	1993	52.38	13.06	Prague	1850	1880	50.08	14.42
Providence	1850	1860	41.68	-71.25	Reykjavik	1820	2001	64.13	-21.90
Riga	1850	1990	56.81	23.89	Rochefort	1862	1881	45.93	-0.93
Rome	1869	1881	41.95	12.50	Scutari	1866	1880	41.00	29.05
Sevastopol	1850	1990	44.61	33.55	Sibiu	1878	1881	45.80	24.15
St Johns	1852	1876	47.56	-52.70	Stockholm	1850	1998	59.33	18.05
Stornoway	1872	1881	58.22	-6.32	St Petersburg	1850	2000	59.93	27.96
Stykkisholmur	1874	2003	65.08	-22.73	Tenerife	1901	2001	28.47	-16.32
Tbilisi	1850	1990	41.68	44.95	Tørshavn	1874	2002	62.02	-6.77
Toulon	1868	1881	43.10	5.93	Uppsala	1722	1998	59.86	17.63
Valentia	1861	1995	51.93	-10.25	Vardo	1861	2003	70.36	31.10
Vestervig	1874	1995	56.77	8.32	Visby	1860	2002	57.63	18.28
Wilna	1850	1990	54.68	25.30	Zagreb	1862	2000	45.82	15.98

Table 1.1: *List of the 86 pressure sites used in EMSLP. The start and end year of the record is given, as well as the latitude and longitude in decimal degrees (negative longitudes are degrees west).*

Homogenisation of land-station data.

To address homogenisation issues we applied broad adjustment factors. Specifically, the monthly means were calculated for each daily series and compared to a reference value [the corresponding ADVICE (Jones *et al.*, 1999) monthly station series or obtained by interpolating from the nearest ADVICE or HadSLP (Basenett & Parker, 1997) grid point]. The difference in monthly means was then used to adjust the daily SLP values. To avoid

jumps in adjustments at the end of each month, a binomial filter was applied. Preference was given to the ADVICE station series where possible.

For the Canadian stations and those in the far east of the EMULATE region a final adjustment was required so that their daily average represented the same 24-hour period as the other series. The Canadian stations are five hours behind central Europe, some of the Russian are four hours ahead. As only daily averages were available for these stations, we were forced to interpolate between the preceding (following) day and the actual day for the Canadian (far Russian) stations.

Many more technical details of the homogenization and adjustments for diurnal cycle issues are discussed in Ansell *et al*. (2006).

Interpolation
In order to create spatially complete fields, Reduced Space Optimal Interpolation (RSOI) was used [see Kaplan *et al*. (2000) and references therein].

For EMSLP an estimate of the sampling error was created by using an average (1961-1990) of the combined marine, land and Superfile sampling error. For the marine observations the sampling error for each month (after Parker, 1984) was calculated, as part of the marine gridding procedure. This was multiplied by the square-root of the number of days. In addition, some account of the errors inherent in the ship observations was taken. A value of 0.25 hPa for geographically random one sigma bias was estimated from the differences between synoptic charts and operational model analyses.

Over land, errors were based on the altitude of the station. An estimate of $h/1500$ as the bias associated with the reduction to mean sea level, where h is the altitude of the station was identified by comparing the pressure reduced to sea level and model analyses at a number of high altitude grid points. Again 0.25 hPa was added (vectorially) to the elevation-related bias, to reflect the random bias error. For grid boxes where the Superfile data were employed, we based the error on the intra-box variability divided by the number of observations in that grid box. Historical synoptic charts were used to estimate the number of observations in each grid box. In regions of zero observations (central Greenland and the far North East) the error was set to the intra-box variability at that grid box.

Following Kaplan *et al.* (1997), EOFs were calculated for each calendar day over just the EMULATE region using a covariance matrix calculated from daily NCEP/NCAR (Kalnay *et al.*, 1996) anomalous fields and applying a fourth-order Shapiro filter (Shapiro, 1971). Kaplan *et al*. (2000) found that in order to obtain a more realistic estimate of the signal covariance and, by association, more realistic theoretical error estimates, it was necessary to re-estimate the signal covariance. After applying a test of consistency, outlined in the Appendix of Kaplan *et al*. (2000), it was found that no correction was required, due, we believe, to the smooth NCEP/NCAR fields from which the covariance matrix was estimated.

Incomplete MSLP fields were then reconstructed using the leading 20 EOFs and the error field. Following Rayner *et al*. (2003), we then blended the 'observations' with the reconstruction.

Summary of results

Comparisons with historical products, such as ADVICE and modern reanalysis products (ERA-40, NCEP/NCAR), indicate that EMSLP is able to reproduce climatological features and extreme events well. Three main issues however have been highlighted. Firstly, smoothing applied during the gridding and quality control procedure has 'flattened' the daily fields. The NAO index calculated from EMSLP however appears to have the correct magnitude (Figure 1.2) and there is some indication that at times the flattening cancels out in a monthly analysis of extreme events (not shown).

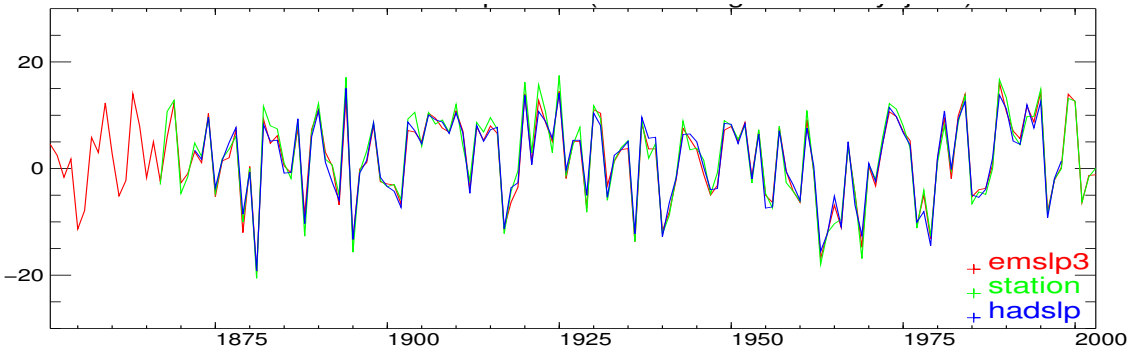

Figure 1.2: *The winter (DJF) North Atlantic Oscillation from 1850-2003 from EMSLP (red, referred as EMSLP3), and HadSLP (blue) gridded products. The winter NAO is calculated by taking the difference between the grid point closest to Ponta Delgada and that closest to Reykjavik. The 1961-1990 mean series value is then removed from each value. Also plotted is a station based index (green), using data from Reykjavik and Ponta Delgada. Differences between the two station series are formed and the 1961-1990 average is also removed; units are in hPa.*

Secondly, during the data sparse period of 1850-1881, the variance to the far east and far west of the EMULATE region is notably lower than in the post-1881 period. This is a consequence of the RSOI procedure and data sparseness. Thirdly, again during this data sparse period, the pressures over Greenland appear to be too high in winter. While it is difficult to correct these problems, error estimates produced with the OI solution can be employed to add error bars. This result also highlights the need to digitise the millions of observations that are still available in ship log books held in the UK National Archives at Kew, London.

Conclusions

Despite these issues, we believe EMSLP will be suitable to characterise circulation patterns over the region. A paper (Ansell *et al.*, 2006) which gives a comprehensive account of the production and testing/validation of the MSLP daily database has been accepted by the *Journal of Climate*. In addition to EMSLP daily database which is a gridded product, individual land-station atmospheric daily pressure series have been made available to all interested parties through EMULATE web pages.

6.3.2 Work Package 2

Scientific achievements

WP leader: Jucundus Jacobeit (UAUGS)

Background

The daily MSLP data set reconstructed back to 1850 within WP1 will be used for analyses relating variations and trends in atmospheric circulation to sea surface temperatures (WP3) and to prominent extremes in temperature and precipitation (WP4). Therefore it is necessary in a preceding step to condense information from WP1 into characteristic circulation patterns. At the same time, basic material is required with respect to the temporal variability of these circulation patterns including indices of within-pattern variability. Therefore WP2 has developed and addressed the following scientific objectives:

Scientific Objectives

- *Define leading atmospheric circulation patterns for two-month and three-month seasons.*
  This includes both the conventional meteorological seasons (DJF, MAM, JJA, SON) and the shorter natural seasons (JF, MA, …, ND) extended in the present context to all over-lapping possibilities (FM, …, DJ).

- *Create a database of quantitative changes in pattern amplitudes since 1850.*
  This depends on the particular type of circulation patterns derived before and includes different approaches which will be discussed below.

- *Assessments of trends in pattern amplitudes and in the incidence of their extremes.*
  For this purpose comprehensive trend matrices have been compiled allowing a complete overview of all overlapping trends and their significance within the entire EMULATE period.

- *Characterise within-pattern variability.*
  For this purpose, appropriate indices have been defined and calculated for moving time windows.

Applied methodology, main deliverables, and scientific achievements

These issues will be discussed according to the above-mentioned objectives with the first three corresponding to deliverables D5, D6, and D10, respectively.

I) Leading atmospheric circulation patterns (→ D5)

A wide range of statistical techniques has been applied including S-mode and T-mode principal component analysis (PCA), nonlinear PCA, k-means cluster analysis (CA), an optimizing cluster algorithm with randomized orders, the simulated annealing technique, and a novel technique merging the last two concepts called SANDRA (simulated annealing using diversified randomized runs). Extensive testing by several partners, in particular the WP leader (UAUGS), the Hadley Centre (MET OFFICE), UBERN and Ian Jolliffe (University of

Aberdeen) including mutual visits at the cooperating institutes, led to the following conclusions: linear PCA – although a strong tool for deriving dynamical modes – suffers from being constrained by orthogonality implying extremely unequal frequencies of dominant realisations of the corresponding circulation patterns (being a serious disadvantage for further investigations in other work packages). Nonlinear PCA (e.g. Monahan, 2001) proved to be constrained – e.g. for the purposes of extremes analyses in context of WP4 – by a systematically low number of resulting circulation patterns. Conventional k-means CA (e.g. Hartigan & Wong, 1979) turned out to be strongly affected not only by the actual starting partition, but also by the order of objects thus indicating a generally missing strategy to avoid local optima of the optimization function. These drawbacks could be eliminated by the SANDRA technique combining a simulated annealing approach (e.g. Lukashin & Fuchs, 2001) with a randomization of orders by carrying out a large number of simulated annealing runs (e.g. 500) each time with different series of random numbers and selecting the result with highest cluster quality. This novel approach was able to avoid local optima reached by chance and ensured a very close approximation of the global optimum in all cases for the different seasons. It was therefore chosen as the most appropriate technique for defining leading atmospheric circulation patterns according to deliverable number 5 (D5) whose results in terms of seasonal cluster centroid patterns are included in the WP2 part of the official EMULATE website:
http://www.cru.uea.ac.uk/projects/emulate/emslp3_pattern_classification/emslp3_pattern_classification/

A major achievement of these studies is the evidence that conventional k-means CA is not sufficient to obtain robust cluster solutions for complex data sets; this is only feasible by more sophisticated techniques like SANDRA which ensure that no persistence in randomly reached local optima will take place (Philipp *et al*., 2006). Complexity in data sets – as given by the daily mean SLP grids back to 1850 – may be defined by the absence of distinctly separated groups of objects inherent in the original data. This might be due to large sample sizes, to the absence of preferred stages of object attributes, or to a huge number of weak distribution maxima in the multidimensional space of attributes. WP2 of EMULATE has succeeded in developing an appropriate technique to classify such complex datasets with optimised robust results.

One crucial point, however, is still remaining: the number of clusters for which the optimisation procedure is applied. Extensive testing has confirmed previous findings that there is no reliable clue to the optimal number of clusters arising from the corresponding techniques themselves (additionally confirmed by recent classification literature, e.g. Stephenson *et al*., 2004). Despite the fact that the optimised cluster centroid patterns are no longer orthogonal, the most reliable clue to the number of distinctly different patterns that fit into the dataset has been given by a T-mode PCA applying an extended version (Philipp *et al*.. 2006) of the dominance criteria (Jacobeit, 1993) ensuring that only those patterns will be extracted that are significantly realised in the data set. This number and the corresponding cluster solution is recommended in the EMULATE website among several cluster solutions being offered additionally. One example out of all D5 results for 16 different 2-month and 3-month seasons is given in Fig. 2.1 referring to the high winter season January/February. Note that cluster centroid patterns are calculated in raw data dimensions whereas the SANDRA technique was applied to area weighted and error weighted MSLP fields: area weights are defined as square roots of the cosine of latitude, the error weight for each grid point is defined as the inverse of the mean optimum interpolation error related to its standard deviation. Thus,

the classification is primarily based on those data with a high reconstruction quality (see Fig. 2.2 with the error weights for the JF season as in Fig. 2.1).

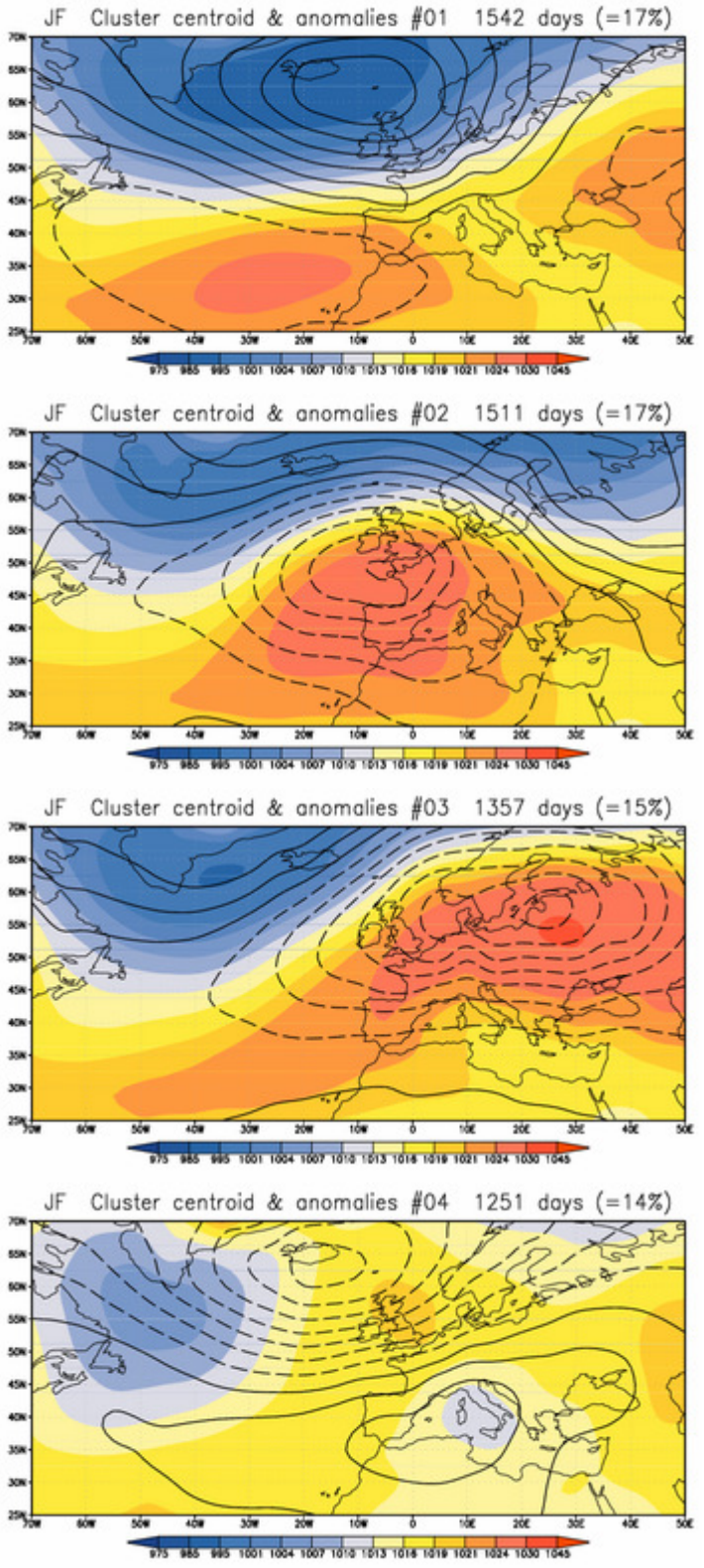

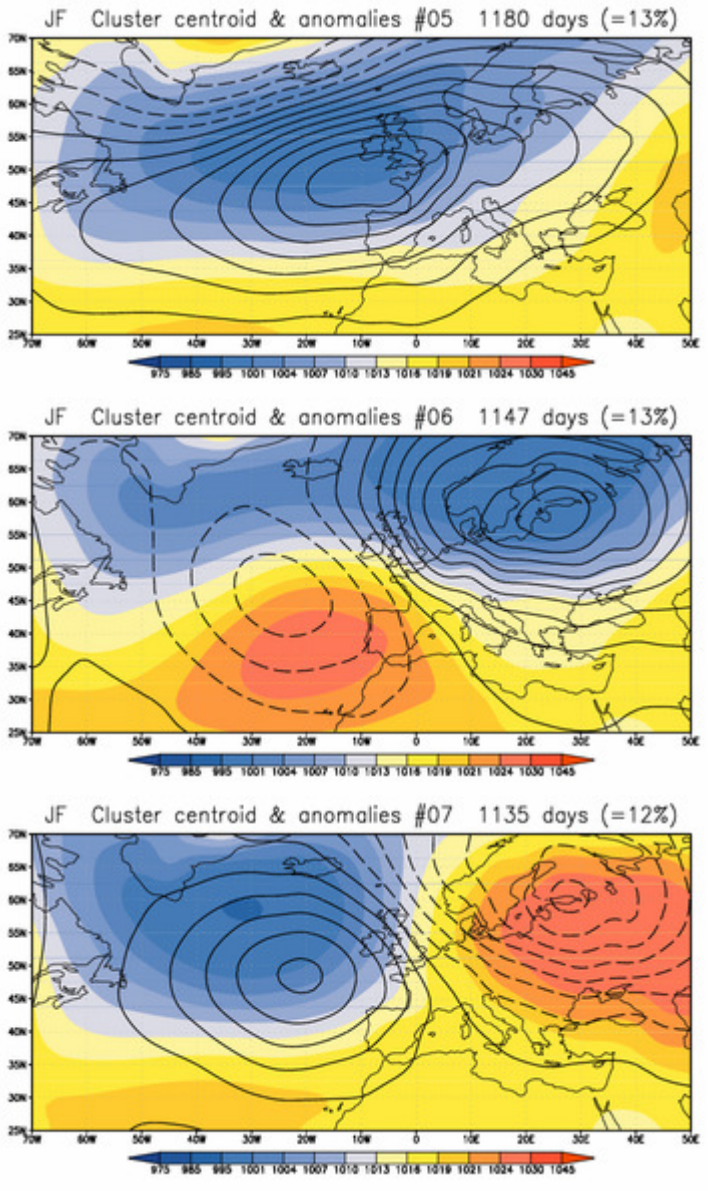

Fig. 2.1: Daily MSLP cluster centroids (recommended solution with 7 clusters, see text) resulting from the SANDRA technique for the January/February season 1850-2003. Colour contours represent the spatial SLP fields in raw data dimensions (hPa without area and error weights), lines show the interpolated grid point anomalies [hPa] referring to the 1850-2003 mean for this season (contour interval 2hPa, values > 0 dashed).

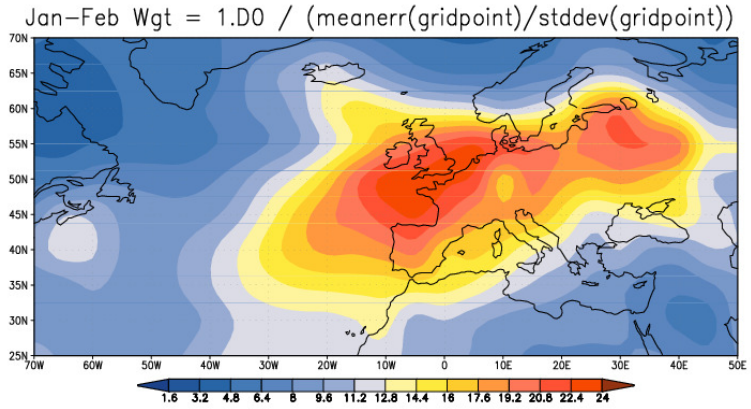

Fig. 2.2: Error weights for the Jan/Feb season applied to the reconstructed MSLP data. The weights are calculated as the inverse of the mean optimum interpolation error for each grid point related to its standard deviation.

The example of leading circulation patterns during January/February (Fig. 2.1) includes two more or less zonal patterns (Clusters 1 and 6) which are, however, predominantly linked with different extremes of climate over Central Europe: Cluster 1 resembling the positive mode of the NAO covers most of the extreme warm winter days, whereas Cluster 6 with its eastward shifted low pressure centre is most important for extreme precipitation events during this season (see the Augsburg contribution to D15 on the EMULATE website). Thus, the daily MSLP classification achieved by the SANDRA technique proved to be highly consistent with particular differences in circulation dynamics known from synoptic climatology. Furthermore, this advanced classification has become part of the COST action 733 dealing with Harmonisation and Applications of Weather Types Classifications for European Regions (Philipp *et al.*, 2005). Thus, it represents significant progress in both methodological development as well as research applications.

The number of clusters determined according to the dominance criteria for T-mode principal components extraction varies with season as specified in Tab. 2.1. These different numbers are consistent with the seasonally varying dynamic conditions in the atmosphere (lowest numbers during summer with its reduced large-scale exchange intensity, largest numbers during the transitional seasons characterized by reorganisations of the large-scale circulation). Since this PCA-based approach has been selected for determining the decisive number of SANDRA cluster patterns, too, an additional classification has been added to the WP2 part of the EMULATE website based on composites for each T-mode PC derived from all those daily MSLP fields having the highest loading on the corresponding PC (compared to all other extracted PCs). Obviously there is a sharper decline in frequencies for these PCA-based patterns than for the SANDRA-based patterns discussed earlier.

T-mode PCA techniques in an extended version have been taken up again in context of WP4 for deriving daily circulation pattern sequences linked to the occurrence of extreme events (see the Augsburg contribution to D15 as well as Jacobeit *et al.*, 2006b).

JF	FM	MA	AM	MJ	JJ	JA	AS	SO	ON	ND	DJ	DJF	MAM	JJA	SON
7	9	11	10	8	5	6	8	10	7	7	7	9	11	6	8

Table 2.1: Number of daily MSLP cluster patterns for the different 2-month and 3-month seasons, 1850-2003 based on the number of extracted T-mode principal components according to the extended dominance criteria (see text).

The SANDRA classification scheme has further been applied in the context of the WP3 analyses deriving daily MSLP cluster patterns for three 50-year sub-periods and thus assessing the degree of non-stationarity in the SLP classification (see the Augsburg contribution to D11). The latter reference also includes temperature and precipitation patterns for the daily MSLP clusters, on a whole-period basis as well as for the three 50-year sub-periods, but restricted to the four conventional 3-month seasons.

Related to D5, though beyond the scope of its particular definition, additional classification analyses have been carried out which were already described in Section 3 of this final report and therefore will only be listed as a complementary summary:

- SANDRA clustering with temperature or precipitation covariates in order to derive SLP patterns with particular climatic characteristics (e.g. warm, cold, wet or dry in a selected region).
- Derivation of a set of 'fringe patterns' to each daily MSLP cluster centroid in order to present a more comprehensive overview of SLP patterns included in each cluster. This pattern range can also be downloaded for each cluster from the WP2 part of the EMULATE website.
- Time constrained clustering aiming at an increased persistence in cluster sequences.
- Clustering objects on subsets of attributes (COSA) with particular focus on regional subsets (Central Europe and the Mediterranean area).
- Objective classification of the reconstructed daily MSLP fields into Central European Grosswettertypes in order to achieve a closer correspondence of circulation patterns to regional extremes in temperature and precipitation. This classification was also applied to some of the WP4 analyses (see the Augsburg contribution to D15).

II) Pattern amplitudes (→ D6)

The most direct way to describe the temporal variability of the D5 cluster patterns would be the calculation of seasonal cluster frequencies (done for example in Philipp *et al.* (2006) for the conventional 3-month seasons, also available as *ASCII* files for all 16 seasons via the EMULATE website). However, daily resolved pattern amplitudes are required for D6, and the first approach to calculate them (realised in the D6 delivery after project month 24, now referred to as the 'old version') consisted of correlating each daily MSLP field (without any latitude or error weighting) with the cluster centroid patterns of the corresponding season. This 'old' version – developed according to the nature of T-mode PCA loadings derived from correlation matrices – suffered from generally high values of these coefficients thus obscuring

differences between the various cluster patterns. Therefore another version has been developed based on Euclidean distances between each daily MSLP field and the cluster centroid patterns, now considering the latitude and error weights applied by the SANDRA clustering technique. These coefficients have further been inverted and normalised and may be seen as appropriate daily amplitudes for the seasonal SLP cluster patterns. Fig. 2.3 gives an example referring to the JF season, i.e. to the cluster patterns of Fig. 2.1 (complemented by low-pass filtered time series and normalised cumulative anomalies). Obviously there are distinct differences in time between the various cluster patterns as may be seen especially from the cumulative anomalies.

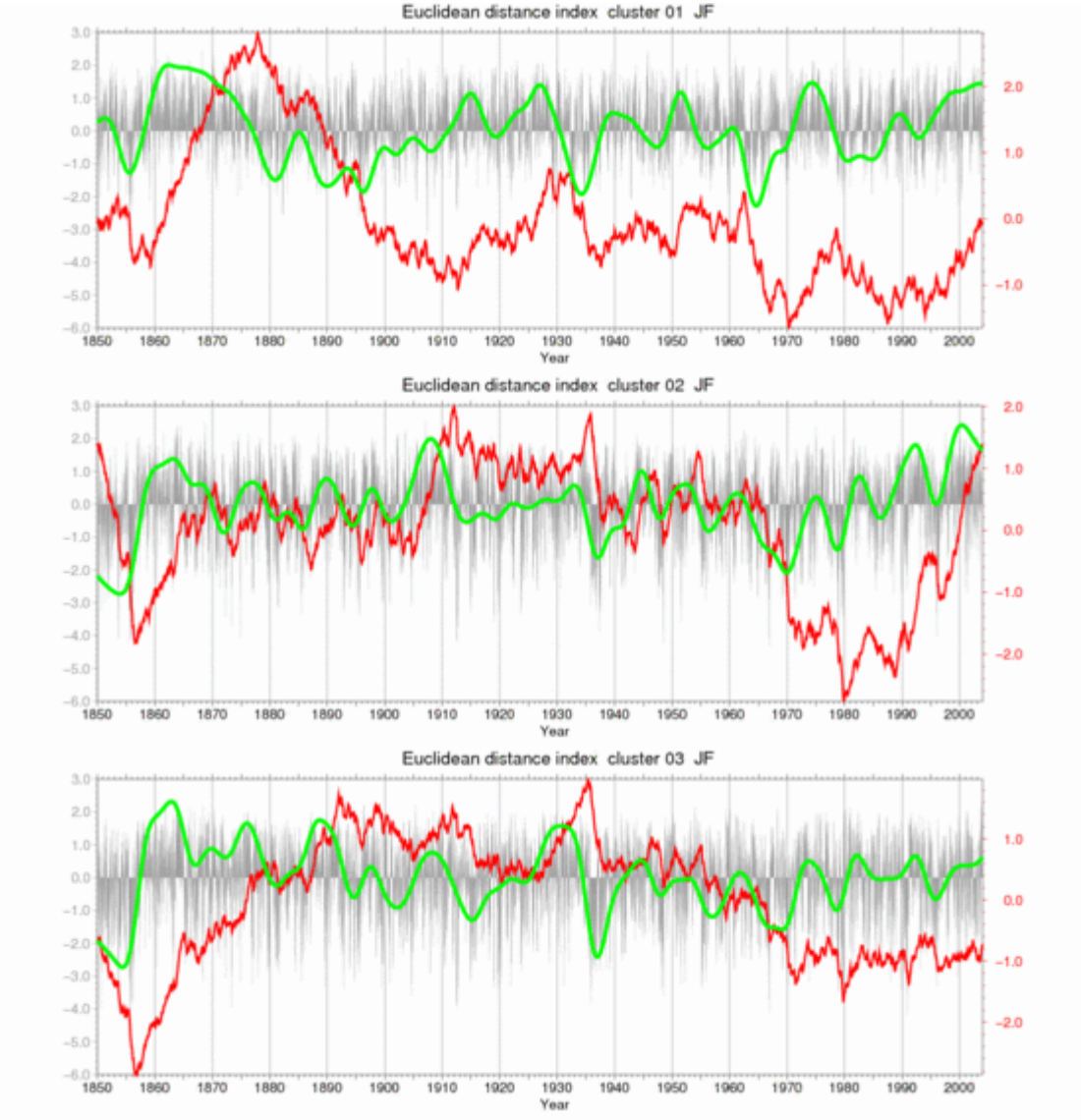

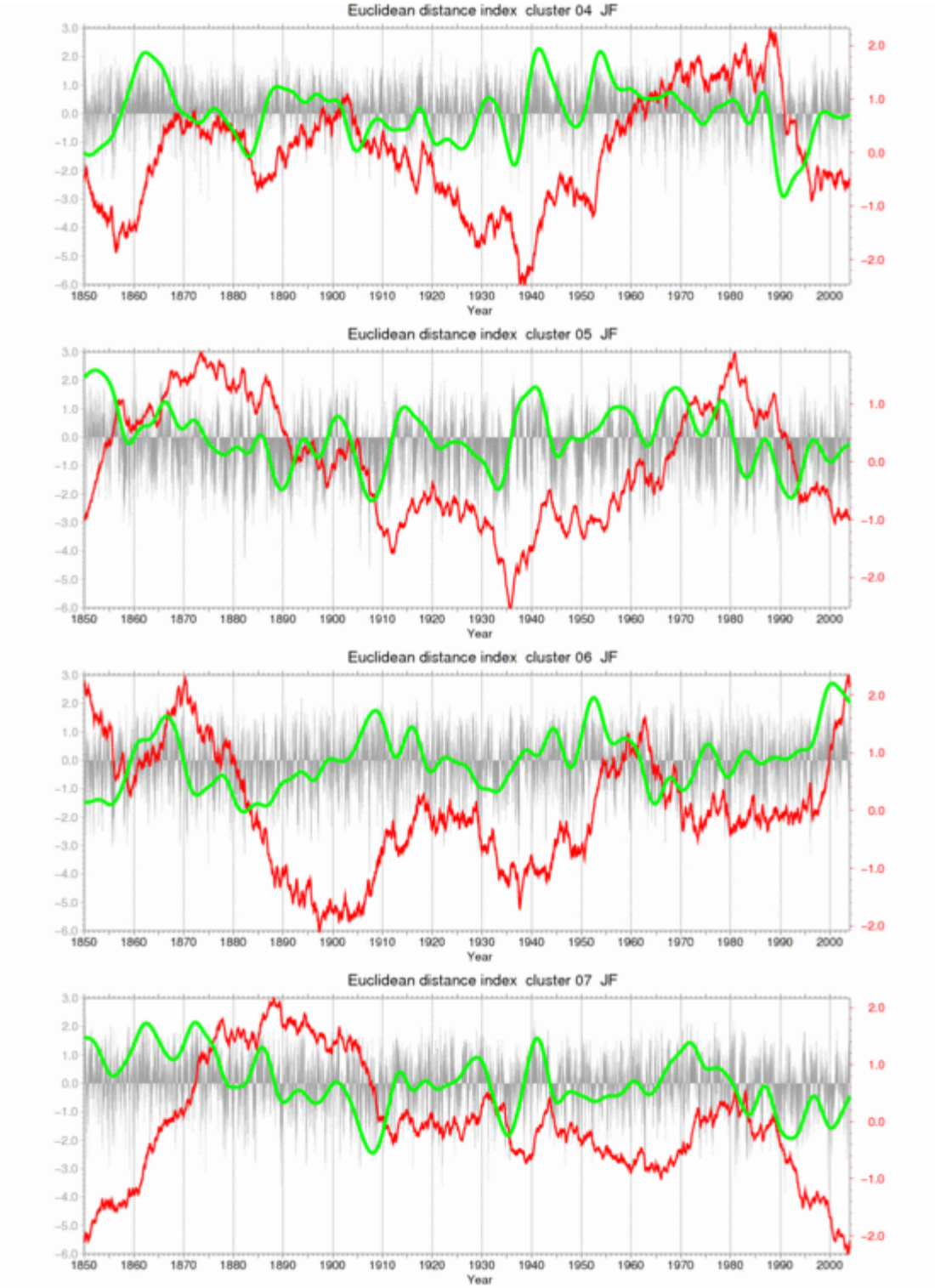

Fig. 2.3: Time coefficients (amplitudes) 1850-2003 for the January/February daily MSLP cluster centroid patterns 1-7 of Fig. 2.1. *Black bars:* inverted and normalized Euclidean distances between the corresponding cluster centroid pattern and the daily MSLP patterns (both latitude and error weighted). *Green line:* low-pass filtered time coefficients. *Red line:* normalized cumulative anomalies of the time coefficients.

On the WP2 part of the EMULATE website another version of daily pattern amplitudes has been added based again on correlation coefficients, but now considering the latitude and error weights and normalising the resulting values (as for the Euclidean coefficients, too, see Fig.

2.3). These newly calculated, correlation-based coefficients show also distinct differences in time between the various cluster patterns (in contrast to the 'old version'), but they do not correspond in general to those from the Euclidean coefficients. This reflects the different nature of these coefficients with the correlation-based ones considering primarily the particular configurations of the SLP patterns and the Euclidean ones (see Fig. 2.3) including absolute pressure differences into the similarity calculations.

Related to D6, though beyond the scope of its particular definition, further investigations with respect to the temporal dimension have been carried out. In particular the work of Linderholm (2006) from UGOT dealing with a paleoclimatic reconstruction of the summer NAO, will be of great importance for further studies extending the temporal domain beyond the EMULATE period back to 1850.

III) Trends in pattern amplitudes and their extremes (→ D10)

These analyses have been carried out at an earlier phase of the third reporting period, therefore the cluster pattern amplitudes are not yet based on the most recent version used for example in Fig. 2.3. Amplitudes submitted to the following trend analyses were defined as non-inverted Euclidean distances thus reflecting growing dissimilarities with the corresponding cluster centroid in the case of increasing amplitude values. Amplitude extremes were defined in terms of particular percentiles (2^{nd}, 5^{th}, 10^{th}, 90^{th}, 95^{th}, 98^{th}), however differences of trend patterns within the groups of lower and of upper percentiles, respectively, proved to remain quite small so that the graphical representations for the WP2 part of the EMULATE website could be restricted to the 2^{nd} and the 98^{th} percentiles for all seasonal cluster pattern amplitudes.

In order to get a comprehensive overview with respect to all possible trends of different duration during the entire EMULATE period 1850-2003, triangular trend matrices (see below) have been compiled including all overlapping trends for periods greater than or equal 20 years: they may be identified by combining all start-years and all end-years on both axes of the matrices. Trends have been calculated both for pattern amplitudes (based on moving 20-day periods) and for their extreme percentiles (on a seasonal basis). All calculated trends have been submitted to the non-parametric Mann-Kendall trend test, insignificant trends are marked by black dots within the matrices. Results for all SLP cluster patterns during all 16 seasons are included in the WP2 part of the EMULATE website, only one selected example is shown in Fig. 2.4.

This example reproduces the amplitude trend matrices for two SLP patterns during winter (DJF). Cluster 1 (a NAO-like pattern, see the EMULATE website) has negative distance-trends (i.e. an increase in patterns similar to the centroid) mainly during the last decades, during earlier periods (e.g. ~1910-1970 or from 1860 onwards) less importance is indicated. Cluster 6 (with a strong Russian high and an Atlantic low) has a long-term positive trend in Euclidean coefficients throughout the EMULATE period associated with its negative trend in seasonal cluster frequencies (Philipp *et al*., 2006) indicating a gradual decline for this Russian high pattern after 1850. This is also reflected in its percentile trends (not shown here). Otherwise, only few significant trends can be observed for the amplitude extremes indicating that they are not strongly linked to low-frequency variability in the corresponding circulation patterns.

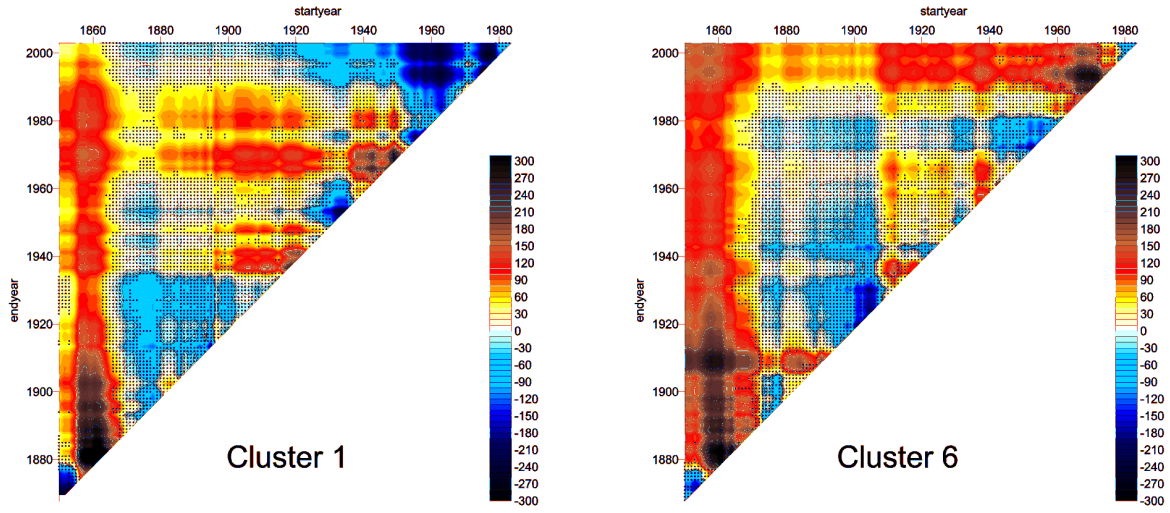

Fig. 2.4: Winter (DJF) trend matrices for the pattern amplitudes (based on non-inverted Euclidean distances) of daily MSLP Clusters 1 and 6. Statistically insignificant trends (95% level) are indicated by dots.

Related to D10, further investigations of trends of circulation indices have been carried out. Della-Marta (2006) from UBERN investigated North Atlantic and European winter cyclone changes from 1881-2003 by applying a Lagrangian cyclone tracking algorithm (Murray & Simmonds, 1991) on the EMSLP dataset (referring to large-scale systems according to the gridded data resolution). Cyclone system density (Fig. 2.5) has also been computed at grid points north and south of the line connecting 45ºN, 60ºW with 55ºN, 30ºW (Bhend, 2005) providing a North-Atlantic storm track index (Fig. 2.6 with positive values for a northern position). The main result is a significant decrease in the number of cyclones in the central North Atlantic and the Mediterranean region from 1881 to 2003 linked with a northward shift of the North Atlantic storm track.

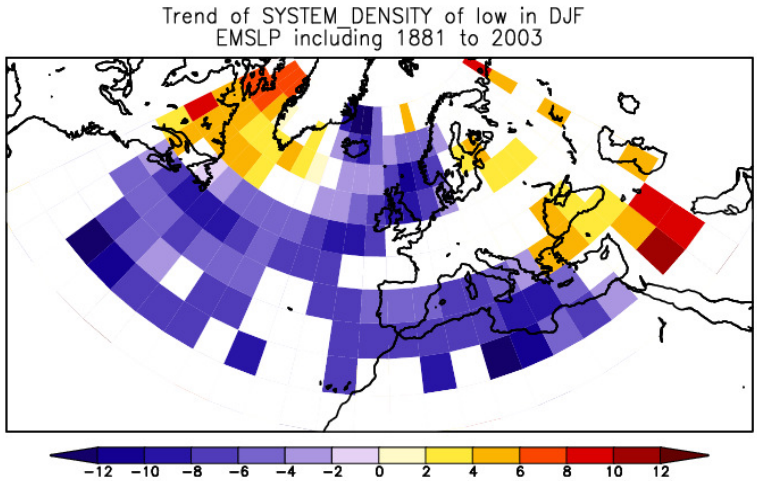

Fig. 2.5: Linear trends in winter (DJF) cyclone system density for the 1881-2003 period.

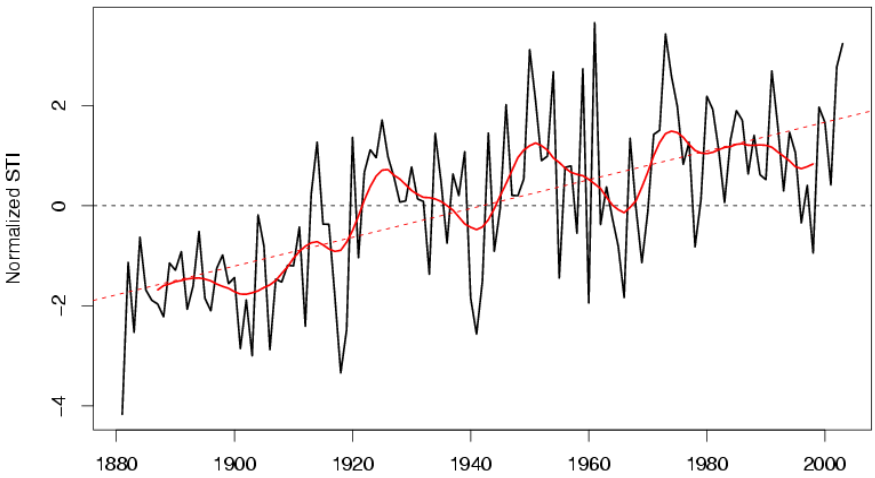

Fig. 2.6: The winter (DJF) North Atlantic storm track index (STI) for the 1881-2003 period (positive values indicate a more northern position).

IV) Within-pattern variability

For its characterization, several parameters (cp. Jacobeit *et al*., 2003) have been calculated on a daily basis: a correlation-based approximation for the relative vorticity within the area 40-60°N, 10°W-30°E; an intensity index measuring the pressure gradients between the corresponding centres of action; a temperature index based on 14 Central European stations, and a precipitation index based on 25 stations from this area. All these indices have been calculated as normalized 31-year moving averages for all the seasonal cluster patterns and are included in the WP2 part of the EMULATE website.

As one winter (DJF) example referring to within-pattern temperatures, Fig. 2.7 shows a distinct impact of global warming with different degrees of intermediate cooling between ~1930 and 1960: for the NAO-like cluster 1 (see the EMULATE website) it remains rather moderate, for cluster 2 with a strong Russian high extending up to the British Isles it goes down to well below-average values, and for cluster 6 with the Russian high extending only up to Central Europe it develops even stronger before the recent warming which reaches peak values for the south-westerly cluster 1.

Another example referring to within-pattern vorticity and precipitation is given in Fig. 2.8. The NAO-like cluster 1 for winter shows increases to higher levels until the 1920s with subsequently larger amplitudes for vorticity than for precipitation. Cluster 7 with a cyclone near Genoa has dropped considerably in vorticity since the 1940s, but within-pattern precipitation turned again already two decades later reaching its highest values at the end of the time series (note its calculation as 31-year mean values).

Already these few examples clearly demonstrate that climate variability is linked not only to frequency changes but also to within-pattern changes of major circulation types (see also Beck *et al*., 2006).

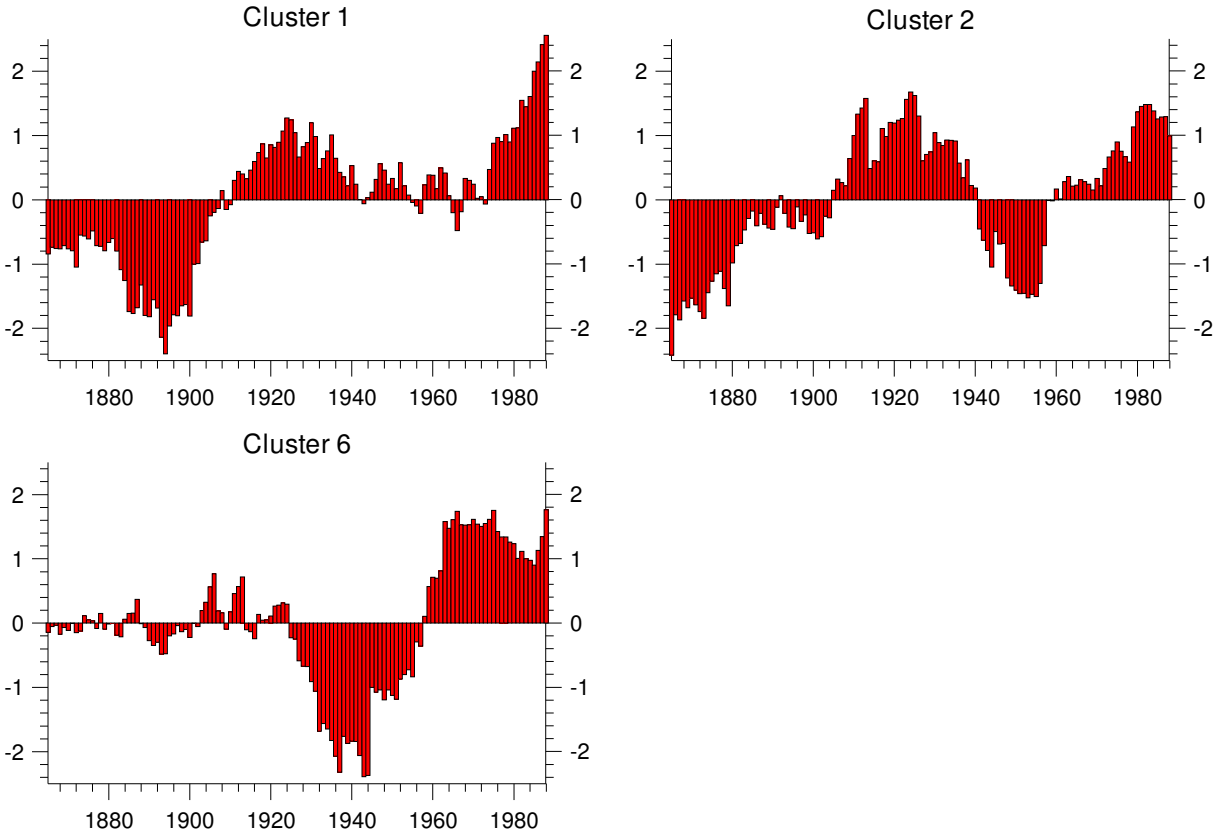

Fig. 2.7: Normalised 31-year moving averages of within-pattern temperature in Central Europe for daily MSLP Clusters 1, 2 and 6 during winter (DJF) 1850-2003.

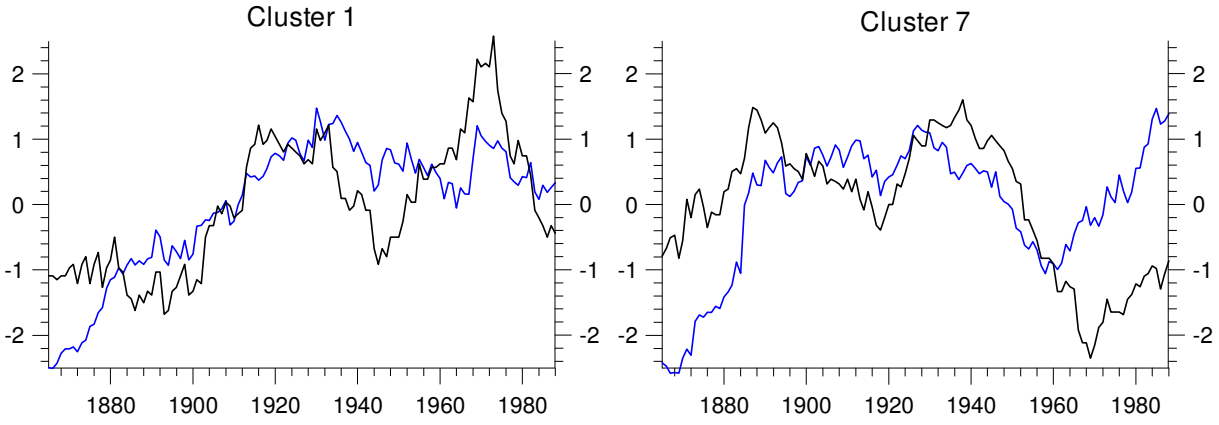

Fig. 2.8: Normalised 31-year moving averages of within-pattern vorticity 40-60°N/10°W-30°E (black lines) and within-pattern precipitation in Central Europe (blue lines) for daily MSLP Clusters 1 and 7 during winter (DJF) 1850-2003.

Conclusions

WP2 has developed a highly sophisticated clustering technique (simulated annealing using diversified randomized runs) being most appropriate for complex data sets like the reconstructed daily MSLP fields back to 1850 from WP1. Using this technique optimised robust clusters have been derived representing in its cluster centroids the leading atmospheric circulation patterns on a daily scale for all 2-month and 3-month seasons of the 1850-2003 period (D5). Besides the seasonal cluster frequencies, daily SLP cluster pattern amplitudes have been determined (D6) based on both Euclidean distances and correlation coefficients, in a final version also considering the latitude and error weights applied in the clustering procedure itself. Generating triangular trend matrices, a complete overview of all overlapping trends in SLP pattern amplitudes and their percentile-based extremes could be achieved (D10). Additionally, within-pattern variability has been assessed by means of several dynamic and climatic parameters indicating that climate variability is linked to this internal forcing by considerable amounts (at least around 50% according to Beck *et al*., 2006). Furthermore, different approaches of extended classification techniques and variability analyses have been tested and evaluated. WP2 results have also been used for first studies on temperature and precipitation extremes (WP4), and these efforts will be extended further in the future.

6.3.3 Work Package 3

Scientific achievements

The overall aim of Workpackage 3 (WP3) was to understand how variations and trends in atmospheric circulation and associated surface climate variability over Europe are affected by sea surface temperature (SST) patterns, particularly those in the North Atlantic, and by natural and anthropogenic forcings. To do this, it was first necessary to document the observed spatial and temporal relationships between SST, mean sea level pressure (MSLP) and associated seasonal European temperature and precipitation patterns (Deliverables D7, D11). The MSLP information, which was on sub-monthly time scales, was provided by WP1 and WP2. A related objective was to develop a gridded drought index data base, and investigate the existence of any links between North Atlantic SST patterns and European-wide drought patterns (D8). The next step was to confirm the observed relationships using atmospheric model simulations forced with historically-observed SST and sea-ice (D12). The influence of other external forcings, both natural and anthropogenic, on the SST-MSLP-European climate relationships was also to be assessed by selectively including these forcings in the model simulations (D13). These studies aimed in particular to highlight similarities and differences between the seasons. A further output of the simulations was to be the quantification of the fraction of the total spatial and temporal variability that can be explained by internal stochastic variability and by all available external forcings respectively. The aim of this was to estimate potential predictability, where feasible, on interannual to decadal time scales (D12).

We summarise the scientific progress in WP3 below, focusing on each deliverable in turn.

Deliverable D7: *Assessment of the variability of the observed North Atlantic and European atmospheric circulation for the last 150 years in relation to SST patterns.*

This study included the use of clusters derived from the daily EMSLP dataset (WP1 and Ansell *et al*., 2006) by the reliable "simulated annealing" technique (WP 2). Using the HadISST1 dataset (Rayner *et al*., 2003), the research confirmed earlier findings (Rodwell and Folland, 2002) that May SSTs could be used to predict the North Atlantic Oscillation (NAO) in the following winter. Also confirmed were strong relationships between the NAO and European winter temperatures (strong NAO → warm in much of Europe) and precipitation (strong NAO → wet north, dry south). The SST-MSLP relationships were used in a successful real-time prediction of a weaker-than-normal phase of the NAO for winter 2005/6 and consequent below normal temperatures over much of Europe: see also Part 6 of the Final EMULATE Report.

As planned, we also investigated the summer NAO (SNAO), which has a similar pattern to the winter NAO but displaced northwards with centres of action near the UK/Scandinavia and Greenland; also its domain of influence is smaller. Historical changes in the strength of the summer and winter NAO patterns appear to be unrelated. The SNAO features strongly in the cluster analysis of EMSLP for high summer (July and August). An increase in anticyclonicity over and around the UK in recent decades led to decreased summer precipitation over the British Isles, northern France and Germany and into Poland, but with increased precipitation further north and south. However this trend appears to have reversed since the mid 1990s.

The study of the SNAO also confirmed an inverse relationship between MSLP near the UK and Sahel precipitation, at least on decadal timescales (Folland *et al*., 1988). As SST is likely to be a common forcing factor (Folland *et al*., 1991), SST - SNAO relationships were investigated. SSTs in the eastern equatorial Pacific and in part of the North Atlantic in June-July appeared to influence the SNAO in July-August on interannual time scales. Warm eastern equatorial Pacific (El Niño) favoured anticyclonicity near the UK (the positive mode of the SNAO).

Finally, we investigated the influence of the El Niño – Southern Oscillation (ENSO) phenomenon on European climate in January to March. Existing studies had yielded contradictory results: our separate investigation of weak and strong El Niño events suggested that this ambiguity may have arisen because the ENSO influence on European climate is non-linear. The nonlinearity was found using NCEP/NCAR reanalysis fields since 1948, and confirmed using MSLP back to 1850 in the EMSLP dataset: the signatures of weak and strong El Niño events were completely different over Europe. Each signature agreed between reanalysis and EMSLP.

Deliverable D8: *Gridded database of drought index for Europe*.

Van der Schrier *et al*. (2006) report research undertaken on European drought. Maps of monthly self-calibrating Palmer Drought Severity Index (scPDSI) were calculated for summer for the period 1901-2002 for Europe (35°N - 70°N, 10°W – 60°E) with a spatial resolution of 0.5° x 0.5°. The recently introduced scPDSI is a convenient means of describing the spatial and temporal variability of moisture availability and is based on the traditional Palmer Drought Severity Index. The scPDSI improves on the Palmer Drought Severity Index by providing values which are consistent over diverse climatological regions. This makes spatial comparisons of scPDSI values on continental scales more meaningful.

An Empirical Orthogonal Teleconnection (EOT) analysis revealed 6 characteristic patterns of drought or moisture, focused respectively i) north of the Caspian Sea, ii) in the Balkans, iii) over northwestern Europe, iv) over Kazakhstan, v) over the Baltic and northwestern Russia, and vi) over southwestern Europe. The sixth pattern resembled the impact of the winter NAO on winter precipitation. The second drought/moisture pattern resembled the impact of the "East Atlantic" winter atmospheric circulation pattern which consists of a north-south dipole of pressure anomalies spanning the North Atlantic from west to east. The other drought/moisture patterns were not closely related to analysed atmospheric circulation patterns or to ENSO.

Over the region as a whole, the mid-1940s to early 1950s stood out as a persistent and exceptionally dry period, whereas the mid-1910s and late 1970s to early 1980s were very wet. The driest and wettest summers on record, in terms of the value of the index averaged over Europe, were 1947 and 1915 respectively; while the years 1921 and 1981 saw over 11% and over 7% of Europe respectively suffering from extreme drought or wet conditions respectively

Trends in summer moisture availability over Europe for 1901-2002 failed to be statistically significant, both in terms of the spatial means of the drought index and in the area affected by drought. Moreover, the analysis did not support suggestions of widespread and unusual drying in European regions over the last few decades.

In an additional study, summer soil moisture status (as measured by the scPDSI) showed useful predictability using indices of antecedent atmospheric circulation based on "simulated annealing" clustering and other techniques. This was especially true of the 3rd EOT affecting northwestern Europe noted above.

Deliverable D11: *Assessment of the time-varying influence of SST and atmospheric circulation on European surface temperature and precipitation patterns.*

For D11 we documented the observed seasonal relationships between atmospheric variables, using new and extended datasets of daily pressure, temperature and precipitation, and an existing, high-quality SST analysis, HadISST (Rayner *et al*., 2003). For analysis of pressure, we used cluster analysis [D5 in WP2; Philipp *et al*. (2006); Fereday *et al*. (2006)] of the EMSLP daily fields (D3 in WP1: Ansell *et al*., 2006), but we also used empirical orthogonal function (EOF) analysis. We began by examining the stationarity of the cluster patterns from the mid- 19th century until the beginning of the 21st century: in both winter and summer we found a high degree of stationarity between the full period 1950-2003 and the sub-periods 1850-1900, 1901-1951 and 1952-2003. However the spring and autumn showed less stationarity.

In winter the NAO shows clearly in cluster analysis and is, as expected, associated with a tripole SST anomaly pattern over the North Atlantic. More than one method of analysis shows this clearly. Both SST and the winter NAO influence each other, with a stronger influence of the NAO on SST than *vice versa*, at least interannually. The summer NAO (SNAO) atmospheric cluster or EOF (see D7) is clearly associated with SST. Interdecadally the SNAO is associated with the Atlantic Multidecadal Oscillation in SST; on interannual timescales it is associated with ENSO. These results mirror the model results in D12, though the observed interannual relationship of the SNAO with ENSO seems stronger than that modelled. There is some evidence that the observed El Niño effect on the SNAO may be stronger than the observed La Niña effect.

The association between the clusters as defined in EMULATE and surface temperature outside winter is rather weak over Europe. In winter the cluster associated with the positive phase of the NAO is associated mainly with warm conditions over central and northern Europe, as expected. The relationship is strong. Such conditions are therefore associated with the positive phase of the SST tripole over the North Atlantic. Most other clusters are associated with cold to near-normal conditions: associations with SST for these clusters have yet to be assessed. There is some evidence for time-variation in the influence of the NAO on European temperature and rainfall, but any causes related to SST have yet to be investigated. There are no trends in Europe-wide drought. However the regional influence of the SNAO on drought as assessed by the scPDSI (D8) needs further investigation, as the phase and strength of the SNAO clearly influences rainfall in northwest Europe, at least in July and August.

Finally, we stress the influence in winter, especially early winter, of often strong warm or cold SST anomalies in the Ratcliffe-Murray region east of Newfoundland. This influence is in addition to the influence of the SST tripole. It was particularly important in the context of the cold European winter of 2005/6 as December 2005 SST anomalies reached 3°C in the Ratcliffe-Murray region. The European winter of 2005/6, and SST influences on it, are currently under investigation and will be reported elsewhere.

The work on drought done under this deliverable is also documented by van der Schrier *et al*. (2006) and is summarised under D8 above.

Deliverable D12: *Results of model experiments to determine if the observed relationships in D7 and D11 are reproduced or can be better resolved using the longer time scales of the coupled model experiments, and an initial study of mechanisms and potential predictability.*

For D12 and D13, we used simulations with the Hadley Centre atmospheric model HadAM3 bounded by historical SSTs and sea-ice extents taken from the HadISST dataset (Rayner *et al*., 2003). In collaboration with the National Institute of Water and Atmospheric Research, Wellington, New Zealand, we completed 6 simulations from 1869-2002 and 12 simulations for 1949-2002 with natural and anthropogenic forcing; along with simulations of the same length with natural forcing only.

Even with observed SST and specified natural and anthropogenic forcings, HadAM3 was unable to reproduce more than a small fraction of the observed increase in the winter NAO in recent decades. However, parallel simulations including stratospheric circulation changes similar to those observed were able to reproduce the increase in the NAO (Scaife *et al.*, 2005). This suggests that future models used to simulate historical European conditions need to include an improved representation of the stratosphere: this will be addressed in the FP6 EU DYNAMITE project. The hypothesis is that, at least on decadal time scales, the stratosphere amplifies the SST tripole influences on the NAO. Current work is also demonstrating significant potential forecast skill from models on decadal timescales (Smith *et al*., 2006). So models with improved stratospheric representation should also be tested for possible benefits to seasonal to decadal forecasting skill for Europe.

In high summer (July and August), the EMULATE simulations reproduced some aspects of the observed relationships (D11) between the SNAO and the Atlantic Multidecadal Oscillation, and between the SNAO and ENSO. So there may be some unexploited predictability of the SNAO and consequent summer droughts over northwestern Europe. Detailed investigation requires localised SST anomaly data and a high-resolution model.

Although the results of D7, using observations, suggested a non-linear influence of ENSO on European winter climate, the simulations were only able to reproduce the "strong" ENSO-related atmospheric circulation pattern over the North Atlantic/Europe and not the different "weak" atmospheric circulation pattern. The response in the model was found to be linear; it appears that the apparent observed non-linearity is an indirect result of the influence of ENSO on the tropical Atlantic.

We found that a higher model resolution and better observational data are required for an accurate examination of North Atlantic cyclone statistics.

An additional multi-century (1400 year) simulation with our coupled ocean-atmosphere model (HadCM3; Gordon *et al*., 2000) revealed statistically significant impacts of the Atlantic Multidecadal Oscillation over Europe in all seasons, with parallel changes in European and African Sahel precipitation. As the Atlantic Multidecadal Oscillation appears to be potentially predictable for several decades ahead (Knight *et al*., 2005), this implies some decadal predictability of European climate.

Finally, we examined changes in extreme precipitation in winter over Europe in the extra HadAM3 simulations forced with observed lower stratospheric wind changes which gave a strongly increasing NAO between 1965 and 1995 (see above). By comparison with the standard EMULATE simulations which had little increase in the NAO, we found substantial increases (decreases) in extreme precipitation in northern (southern) Europe, in good quantitative accord with observations.

The results of D12 imply that, to interpret past climatic changes over Europe, seasonally-specific influences of natural modes of atmospheric and oceanic variability such as the Atlantic Multidecadal Oscillation (oceanic) and the winter or summer NAO (atmospheric) must be taken into account. To better understand the causes of changes in such primary modes of climate variability is a key aim for the next few years.

Deliverable D13: *Assessment of the relative influence of external forcing factors (natural and human) and internal variability and their seasonal differences.*

We examined two ensembles of climate model simulations, both forced with observed SST and sea ice extent but each having different sets of radiative forcing factors: one had only the major natural forcings and the other had both natural and anthropogenic forcings. Comparison of these two ensembles of simulations has allowed, within the limits of statistical uncertainty, some influences of the effects of anthropogenic forcings on European climate, including circulation, to be evaluated. The methods used here are strictly those applicable in the presence of a common SST forcing and so measure the direct effects of anthropogenic forcing, not the total effects (Sexton *et al.*, 2003), but do allow for the common natural forcing including oceanic natural forcing.

The simulated temperature over Europe, averaged over 1951-2000, was reduced by an average of about 0.5°C by anthropogenic forcing, owing to the cooling effect of anthropogenic aerosols. Thus, Europe responded differently from much of the rest of the globe, which showed mean anthropogenic warmth over this period. The effect appeared strongest in Eastern Europe in the cold half of the year, but in Western and Southern Europe in the warm part of the year. However northern Scandinavia was warmed in winter by anthropogenic forcing. These patterns can be understood by the action of anthropogenic aerosols in reflecting solar radiation; for most of Europe, the largest cooling occurs in summer, when the solar radiation peaks. In Eastern Europe there is a snow-cover feedback on temperature, maximising the cooling there in winter.

The simulated anthropogenic coolness over Europe tended to diminish after about 1980. This is consistent with the mean European climate forcing, which had a minimum in the 1960s. Of course, by using simulations with observed SSTs we can only detect the part of the anthropogenic effect that does not come from SST. Nevertheless, the greater size of the negative forcing signal over Europe compared to the positive signal globally suggests that SST effects by no means dominate. Further tests to quantify this fully are required using coupled models or hybrid “Pacemaker” experiments with models that are largely coupled that can allow for oceanic natural variability as discussed in D13.

Although the role of aerosols has diminished, and future forcings are expected to be dominated by greenhouse gases, these results show that it is important to take into account aerosol cooling when attributing past European climate variability, e.g. the cold winters of the 1960s. Uncertainty in the amount of cooling might arise from SSTs and from the

representation of aerosol in the model. This uncertainty is not large enough, however, to overturn the basic result of a likely anthropogenic cooling in European climate in the latter half of the 20th century.

Overall atmospheric circulation responses in the model, as measured by ensemble differences in MSLP for 1951-2000, showed the largest changes in summer and smallest changes in winter. In summer the main anthropogenic effect appeared to be a pattern over North West Europe similar to that associated with the negative phase of the observed SNAO. Impacts in winter were less significant, although there appeared to be significant increases in MSLP over Western Europe. The lack of significant forced signals in winter shows the importance of internal variability in that season. Winter MSLP trends, like those of temperature, acted to reduce the time-mean differences, whereas summer trends had quite different patterns to the 50-year means. This arose because European atmospheric circulation can respond to remote forcings, whereas temperature is more constrained by the regional radiation balance. The modelled anthropogenic effects on precipitation largely mirrored those in MSLP, with elevated precipitation associated with reduced MSLP. Signals varied through the year, with perhaps the largest effect in high summer (JA), which showed higher precipitation throughout Western and Southern Europe. There were no significant anthropogenic trends in precipitation.

Anthropogenic impacts on circulation in the simulations were also examined using the EMULATE circulation type classification developed in WP2. Mean 1951-2000 circulation type frequencies showed the largest effects in the warmer seasons. Of particular note was a shift favouring negative SNAO in high-summer (JA) with anthropogenic forcing. Differences in trends in circulation type frequency, however, were not significant overall, suggesting considerable internal variability in circulation type frequency. This view was confirmed by a General Linear Model analysis, which failed to relate atmospheric circulation frequency changes to global mean anthropogenic forcing, despite showing a clear link between global mean temperature and forcing. However, this test may reveal more if applied using the European regional forcing.

We also attempted to diagnose the effects of natural forcings in our simulations. A superposed epoch analysis showed summer cooling of order 0.4 °C over Europe in the first and second years after the year of a major tropical explosive eruption. We did not find a winter signal in our simulations. For circulation, there was little suggestion of a change in the simulated frequencies of circulation types. Correlations of European ensemble mean temperature with the 11-year solar cycle showed an effect in summer of a few tenths of a °C. We found no significant solar cycle effect, however, on atmospheric circulation.

Overall, the most significant forced signals found in this study were in the warm seasons, particularly in JA. Particularly noteworthy were changes in the SNAO. So we examined possible future changes in the SNAO in double and quadruple CO_2 experiments using a fully coupled climate model. Progressive changes in the SNAO were found with increasing CO_2 that would be associated with increased summer MSLP over North West Europe. This suggests a heightened risk of summer droughts in this region in the future additional to the effects of the warming on soil moisture alone.

The results here are only from a single model so may be model-dependent. Increased understanding of the role of forcings on circulation requires analysis of responses in other models. It would also be useful to quantify the total effect of anthropogenic SST changes on

European climate so far, for example using coupled model or Pacemaker simulations. Single-forcing simulations may resolve uncertainties over the individual attribution of apparently correlated climate signals. Finally, in EMULATE we have taken the approach of seeking the variability and change in European circulation and then relating it to the major outside influences in the climate system, such as climate forcings, North Atlantic SSTs, and ENSO. Another approach might be to study variability and change in these principal global phenomena and then ask how they relate to European climate.

Conclusions

WP3 has yielded substantial advances in analysis and interpretation of temperature and precipitation over Europe in relation to regional atmospheric circulation and to sea surface temperature in the Atlantic and further afield, especially in winter and summer. Typical patterns of drought and moisture are now better understood in the light of characteristic patterns of mean sea level pressure and their connected oceanic temperature signals. WP3 has enabled improvements in seasonal prediction, and the potential for such predictions is now clearer. However, model simulations have demonstrated the need for a much improved representation of the stratosphere for winter seasonal climate prediction and for simulation of long term trends in winter climate over Europe. The simulations have begun to unravel the anthropogenic influences on European climate, especially in summer, and suggest a tendency to substantrially more frequent drought in future under increasing greenhouse forcing, especially for regions affected by the summer North Atlantic Oscillation.

6.3.4 Work Package 4

Scientific achievements

EMULATE has analyzed changes in observed temperature and precipitation extremes in Europe since the late 19th century. The significance of the atmospheric circulation for the occurrence of such extremes has been assessed. Furthermore, the likely human influence on both extremes and mean values of temperature and precipitation has been determined from ensemble simulations with an atmosphere model.

Assessments of changes in temperature and precipitation extremes since the late nineteenth century (D9 and D14)

To enable analyses of changes in temperature and precipitation extremes, EMULATE has developed a data base, for 230 European stations, with daily temperature and preciptation records going back at least to 1900. There were three main sources; (i) publicly available data bases, (ii) digitization of original data and (iii) personal contacts with data holders in many countries. Locations of all stations are shown in Fig. 4.1. As part of EMULATE, data from 22 sites in Spain have been digitized from the original documents. These Spanish series have been subject to quality controls and data homogenization, including correction for artificial changes due to shifts from early to modern thermometer screens (Brunet *et al*., 2006). The effect of undertaking homogenization is illustrated in Fig. 4.2. EMULATE has also developed a new method for homogenizing daily temperature data, which is capable of adjusting the mean, variance and skewness of daily temperature data (Della-Marta and Wanner, 2006). EMULATE has applied the Della-Marta/Wanner method to a subset of 26 of the temperature series, and some analyses reported here are based on these homogenized station records.

EMULATE has defined 64 climate indices derived from the 230 daily temperature and/or precipitation series. The majority measure some aspect of climate extremes, while a few reflect mean conditions. Software has been developed and used to calculate, for each station, time series of each index for the four traditional climatological seasons (DJF, MAM, JJA, SON) and for all twelve two-month seasons Dec-Jan, Jan-Feb, etc. Data files containing all index time series for each station are available on the EMULATE web site www.cru.uea.ac.uk/cru/projects/emulate/, together with software documentation, information about the file structure and definitions of all indices. A summary of all indices is given in Table 4.1.

Trends in all 64 indices have been calculated over the periods 1801-2000, 1851-2000 and 1901-2000, for all stations that meet certain criteria for data completeness (Chen *et al*., 2006). Over the last century, when data are most complete, the result broadly shows that warming has dominated changes in the upper tail of the distribution of daily temperature data. The lower tail, however, shows cooling trends at a number of sites. This implies a change in shape of the distribution, which affects warm and cold extremes in different ways. A detailed analysis of a subset of 19 indices for summers and winters during 1901-2000 is made by Moberg *et al*. (2006). Average trends (Fig. 4.3), for 75 stations west of 20ºE, show a warming for all temperature indices. Winter has on average warmed more (~1.0 ºC) than summer (~0.8 ºC). Overall, the warming of daily Tmax in winter was stronger in the warm tail than in the cold tail. For summer, there is an overall tendency for stronger warming, both for Tmax and Tmin, in the warm than in the cold tail only in parts of central Europe. Winter precipitation totals, averaged over 121 stations north of 40ºN, have increased significantly by ~12% over

the century. Trends in 90th, 95th and 98th percentiles of daily winter precipitation have been similar. No overall long-term trend occurred in summer precipitation totals, but there is an overall weak (statistically insignificant and regionally dependent) tendency for summer precipitation to have become slightly more intense but less common. There are, however, large regional differences in both temperature and precipitation trend patterns (Fig. 4.3).

Some indices of particular importance for society have been analysed more closely, in particular summer heat waves and the length of the growth season. Using 54 homogenized daily maximum temperature series from western Europe, the change in frequency, persistence and variance of extreme summer temperatures have been investigated (Fig. 4.4). The length of summer heatwaves over western Europe has doubled during the period 1880 to 2003, and the frequency of hot days has increased by 173% (Della-Marta *et al*., 2006a). The heat wave index (like all indices) reveals interannual and decadal variability superimposed on the trend. Therefore, the result of trend analysis is dependent on the choice of analysis period. EMULATE has studied the significance of this for two chosen regions, Germany and Greater Alpine, by exploring certain diagrams called trend matrices (Jacobeit *et al*., 2006a). An example for the Greater Alpine region (Fig. 4.5) shows that the magnitude of warming trends in daily mean temperatures in summer has been particularly large over the last few decades, in line with the recent increased frequency and length of summer heat waves in this region. Another aspect of warming is the increased length of the growth season, which has been studied for the Baltic region and is found to be robust to different definitions of growth season (Linderholm *et al*., 2005)

Assessments of the influence of atmospheric circulation variations on the incidence of extremes (D15)

EMULATE has investigated the influence of variations in atmospheric circulation patterns on the incidence of temperature and precipitation extremes, by using various regression or correlation methods. Overall, the analyses demonstrate that changes in dynamical modes of variability are crucial in explaining observed changes and variability in climate extremes. It is also seen that different regions are influenced in different ways, and that relationships that affect warm extremes not necessarily affect cold extremes with the same strength.

As concerns the causes for observed changes in summer heat waves over western Europe, additionally the patterns in sea surface temperatures and precipitation (as a proxy for soil moisture) were also considered as potential candidates (Della-Marta *et al*., 2006b). Using Canonical Correlation Analysis, heat waves over western Europe are shown to be related to anomalous high pressure over Scandinavia and central western Europe (Fig. 4.6). We also find statistical evidence that long-term changes in the Azores High, continental European Sea Level Pressures (SLP), North Atlantic SSTs and European summer precipitation have driven at least a part of the increased heat wave occurrence. Changes in atmospheric circulation in summer alone is, however, not sufficient to explain the warming trend in summer temperatures. The latter is demonstrated in another analysis that relates the most prominent circulation patterns from the SANDRA (see section 6.3.2 on WP2) clustering technique to temperature changes in central Europe (Philipp *et al*., 2006). Observed linear warming trends during 1851-2003 can be reproduced by up to one third or one half of the total trend for winter, spring and autumn - but not in summer. Nevertheless, seasonal SLP cluster frequencies can explain 34% of summer temperature variance in central Europe (and 59% in winter).

Another study focussed on correlations between the leading mode (EOF1) of daily SLP in each season and 25 of the 64 temperature and precipitation indices for about 130 stations across Europe (Mohammad *et al*., 2006). A clear patern, with significant correlations is found in winter for all indices. In the other seasons, the correlations are mostly weaker but still significant in many cases for some regions. Examples for summer and six of the indices are shown in Fig. 4.7. In this season, the leading SLP mode shows an anomaly centered over the North Sea. High pressure anomalies over this region are significantly associated with high daily maximum temperatures and with positive anomalies in the upper tail of the distribution of Tmax in the region surrounding the North Sea, but there is no significant correlation with variability in the cold tail of Tmax in the same region. The leading SLP mode in summer is also significantly correlated to dryness, reflected in the mean precipitation, to heavy daily precipitation as well as the length of dry spells.

Further related analyses have focussed on two particular regions: Germany and Europe south of 60ºN and west of 35ºE. One study for Germany analyses the importance for temperature and precipitation extremes of circulation patterns derived from daily MSLP classifications, based both on cluster analysis and Grosswetterlagens. Another study specifies major circulation patterns during five-day sequences linked to the extremes by means of extended principal component analyses. It is demonstrated that within-type variations of large-scale circulation types plays an important role in the relationships between circulation and climate extremes. Using yet another approach, the conditional probability that a temperature extreme occurs within a certain atmospheric circulation type has been estimated on a five-grade scale, for each station south of 60ºN and west of 35ºE. Examples of results from these studies are shown in Fig. 4.8.

Assessment of the likelihood of any anthropogenic influence on extremes (D16)

The Hadley Centre atmosphere model HadAM3 has been run with and without anthropogenic forcing to identify possible anthropogenic signals in the statistics of extreme climate events. Daily near-surface air temperature (Tmin, Tmax, Tmean) and precipitation from 36 model integrations have been used to calculate 11 of the 64 EMULATE climate indices, for the DJF, MAM, JJA and SON seasons. An ensemble (for details see section 6.3.3 on WP3) consisting of 18 integrations include both anthropogenic and natural (ANTNAT) forcings, and another ensemble with 18 integrations include natural forcing only (NAT). Here, results from all these simulations are analysed for the period 1951-2000.

The purpose of comparing ANTNAT with NAT runs is to identify an eventual anthropogenic signal. This is done by subtracting results of the NAT runs from those of ANTNAT runs. To minimize the effect of internal variability of climate, ensemble means of all runs in each ensemble are used. The difference in the ensemble means would then reflect the mean impact of the anthropogenic forcing over the period analysed. Furthermore, the difference in trends between ANTNAT and NAT runs would reflect the trend due to the anthropogenic forcing. Results for all 11 indices and all four seasons are shown by Chen and Walther (2006). Examples for JJA are selected in Fig. 4.9.

The two analyses (differences in means and differences in trends) give distinct results. The differences in trends are mostly positive for all indices and all seasons. This clearly indicates that the anthropogenic effect over Europe, in the simulations, has been towards an increased

warming and wetting that affects extremes as well as the means. Most of the differences in trends are, however, not statistically significant. The comparison of the means during 1951-2000 gives another impression. In many cases, ANTNAT is colder than NAT, and these differences are often statistically significant. However, results vary among indices and seasons. The colder ANTNAT conditions are most clearly seen in spring and summer, particularly over much of central Europe. In other regions there are also significant positive differences for some indices. Precipitation indices also show regional variations. For example, PREC95P in summer is significantly drier in ANTNAT over much of northern Europe, but significantly wetter in the Mediterranean.

The generally cooler European conditions in ANTNAT are consistent with the diagnosed forcing in the model simulations, which shows change of ~ +0.5 Wm-2 (in 1950) globally but ~ -1.5 Wm-2 (also 1950) over Europe, resulting from the inclusion of anthropogenic forcings. Comparing the global distribution of forcing change with that of anthropogenic aerosol shows that the forcing reduction over Europe is clearly the result of sulphate aerosols. The effect of the total anthropogenic forcing over Europe is thus rather complex; a cooling on average during 1951-2000 but with increased warming trend towards the end of the twentieth century. Hence, detection of the influence of the anthropogenic forcing, based on model-observation comparisons, is far from a trivial exercise. A detailed analysis of this highly important issue need to be undertaken in the future, beyond the EMULATE project.

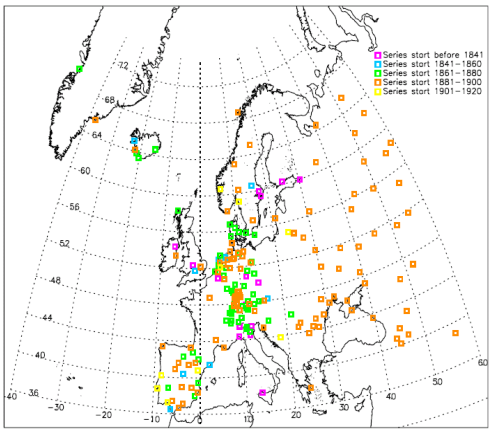

Fig 4.1. Location of EMULATE stations with 100-yr + daily temperature and precipitation records

name	unit	TN	TX	TG	PREC	Description	indices
MEANTN, etc	°C	x	x	x	-	arithmetic mean of TN, TX, TG (TG = TMEAN)	3
PRECTOT	mm	-	-	-	x	precipitation total	1
TN10P, etc	°C	x	x	x	-	2%, 5%, 10%, 90%, 95%, 98% - percentiles	18
PREC90P, etc	mm	-	-	-	x	90%, 95%, 98% - percentiles	3
TN10N, etc	days	x	x	x	-	No. of days below (or above) the corresponding percentile (2, 5, 10 or 90, 95, 98)	18
R90N, etc	days	-	-	-	x	No. of days above the corresponding percentile (90, 95, 98)	3
R90T, etc	%	-	-	-	x	percentage of total precipitation falling above the corresponding percentile (90, 95, 98)	3
R90AM	mm	-	-	-	x	sum of precipitation amount falling above the corresponding percentile (90, 95, 98)	3
SDII	mm	-	-	-	x	simple daily intensity (including only raindays ≥ 1mm)	1
SDII90	mm	-	-	-	x	simple daily intensity for raindays above the corresponding percentile (90, 95, 98) (including only raindays ≥ 1mm)	3
HWDI	days	-	x	-	-	number of consecutive days with more than +5°C above the long-term mean of TX	1
WSDI90	days	-	x	-	-	warm spells: at least 6 consecutive days with TX exceeding the 90% percentile	1
CSDI10	days	x	-	-	-	cold spells: at least 6 consecutive days with TN below the 10% percentile	1
GSL	days	-	-	x	-	growing season length; days between the first and the last period of 6 consecutive days with TMEAN >= 5°C during one year	1
R5d	mm	-	-	-	x	greatest 5-day total rainfall	1
R1d	[mm]	-	-	-	x	greatest 1-day total rainfall	1
CDD	[days]	-	-	-	x	maximum number of consecutive dry days (PREC < 1mm)	1
FD	[days]	x	-	-	-	number of frost days (TN < 0°C)	1
						Σ	64

Table 4.1. Indices for temperature and precipitation extremes and mean conditions

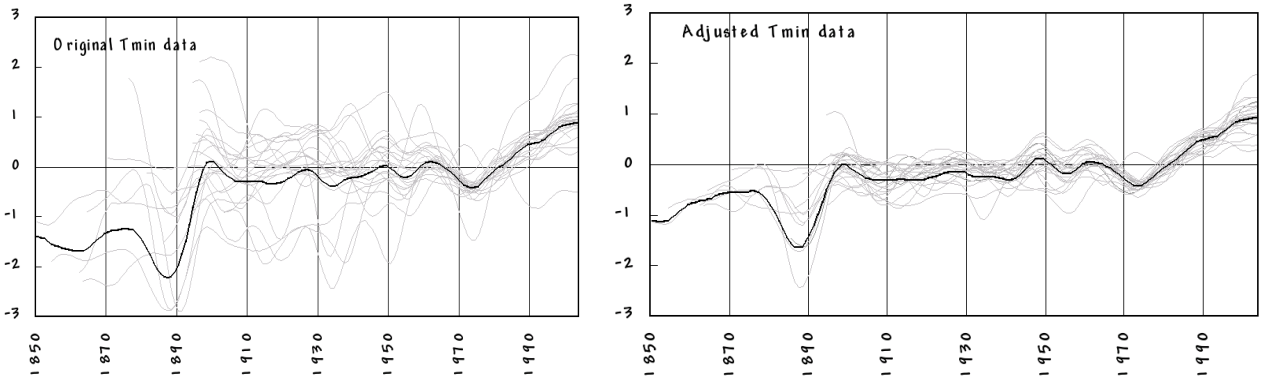

Fig 4.2. Original and adjusted daily minimum temperature series for 22 Spanish stations. Individual sites are grey with the regional average in black.

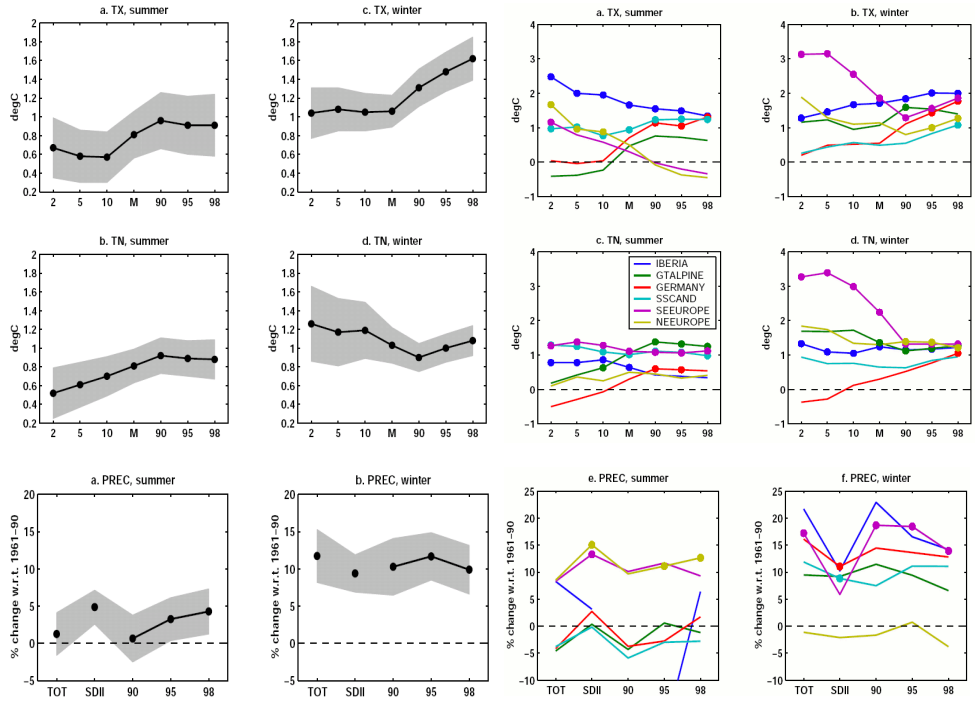

Fig 4.3. Average trends in 19 selected indices over 1901-2000, representative for large parts of Europe (black) with 95% confidence intervals (grey) and for six sub-regions (colours). Dots in the regional analysis indicate trend significance at the 5% confidence level.

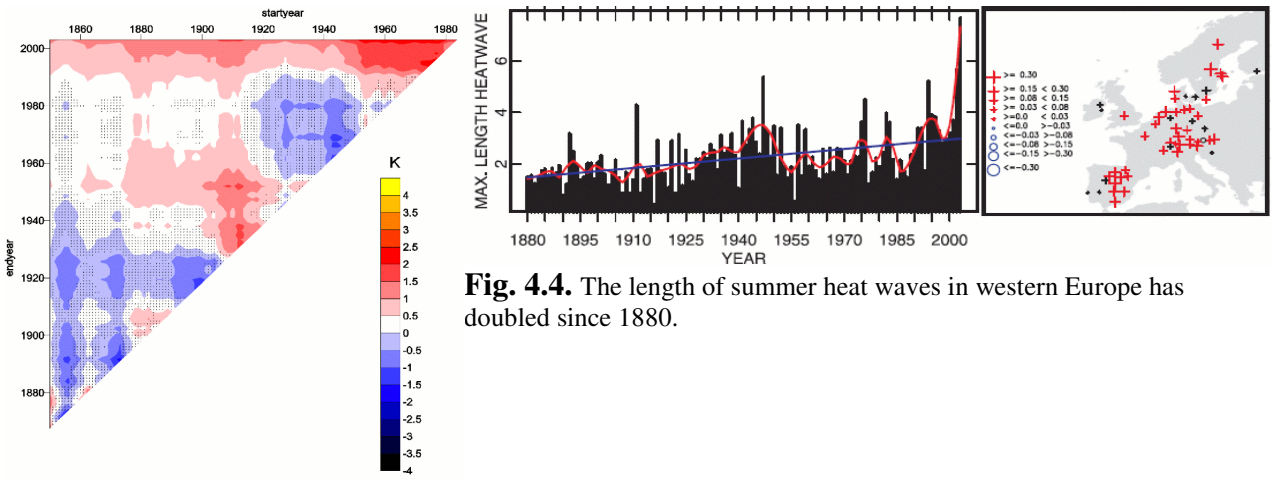

Fig. 4.4. The length of summer heat waves in western Europe has doubled since 1880.

Fig. 4.5. Trends in daily mean temperatures in summer in the Greater Alpine region for all combinations of start and end years. Insignificant (95%) trends are marked with black dots.

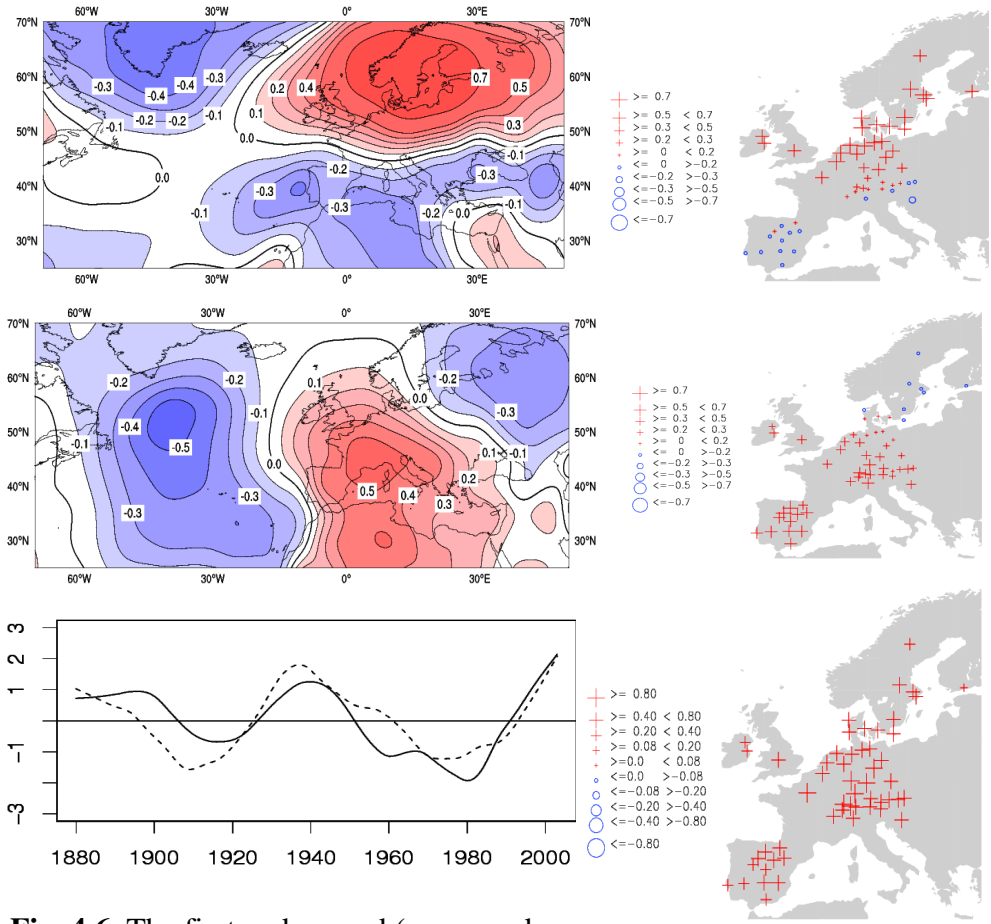

Fig. 4.6. The first and second (upper and middle panel) CCA between JJA averaged SLP and the JJA heat index; SLP canonical patterns to the left and heat wave canonical patterns to the right. Lower panel: (left) time series of smoothed Atlantic Multidecadal Oscillation (dashed) and the first PC of the heat wave data. (right) Loading pattern of unsmoothed PC1 of heat waves.

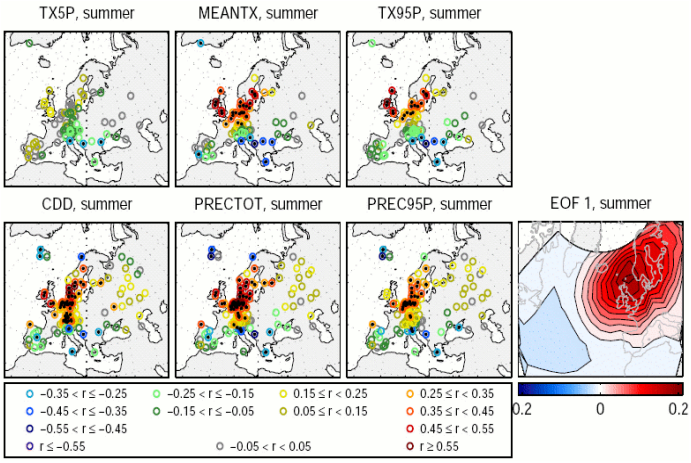

Fig. 4.7. Correlations between the first EOF (to the right) of daily SLP in summer (JJA) and six selected temperature or precipitation indices (the six other maps). Black dots indicate significance at the 1% level. The colours for CDD (Consecutive Dry Days) are inverted compared to the legend.

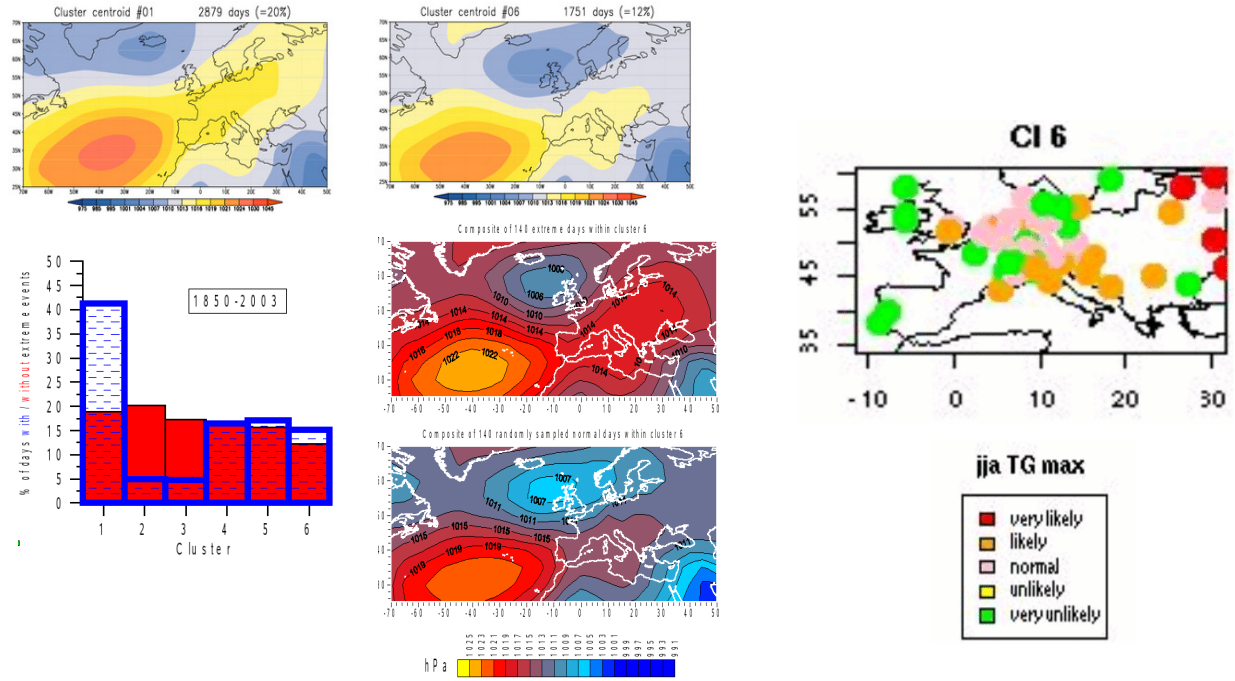

Fig. 4.8. Examples of analyses of relationships between climate extremes and the atmospheric circulation. The two upper maps show Cluster centroid #01 and #06 for daily SLP data in the JJA season (from the SANDRA classification). The histogram shows how the percentage of days with extreme (above 95th percentile) and non-extreme daily mean temperature in summer, for the German region, are distributed among the six clusters. Extreme days are particularly likely to occur in days belonging to cluster #01. Extreme warm summer days also have an enhanced tendency to occur in days belonging to cluster #06. The two lower maps in the center panel show daily SLP composites for summer days with extreme and non-extreme daily mean temperatures, respectively, for days belonging to cluster #06. A strengthening of the high pressure ridge towards the continental Baltic is seen for the extremes composite. The rightmost map shows the likelihood of occurrence of extreme warm summer days at different stations across parts of Europe, under the condition that the days belong to cluster #06. More examples are found in reports by Jacobeit *et al.* (2006b) and Yiou and Fauchereau (2006).

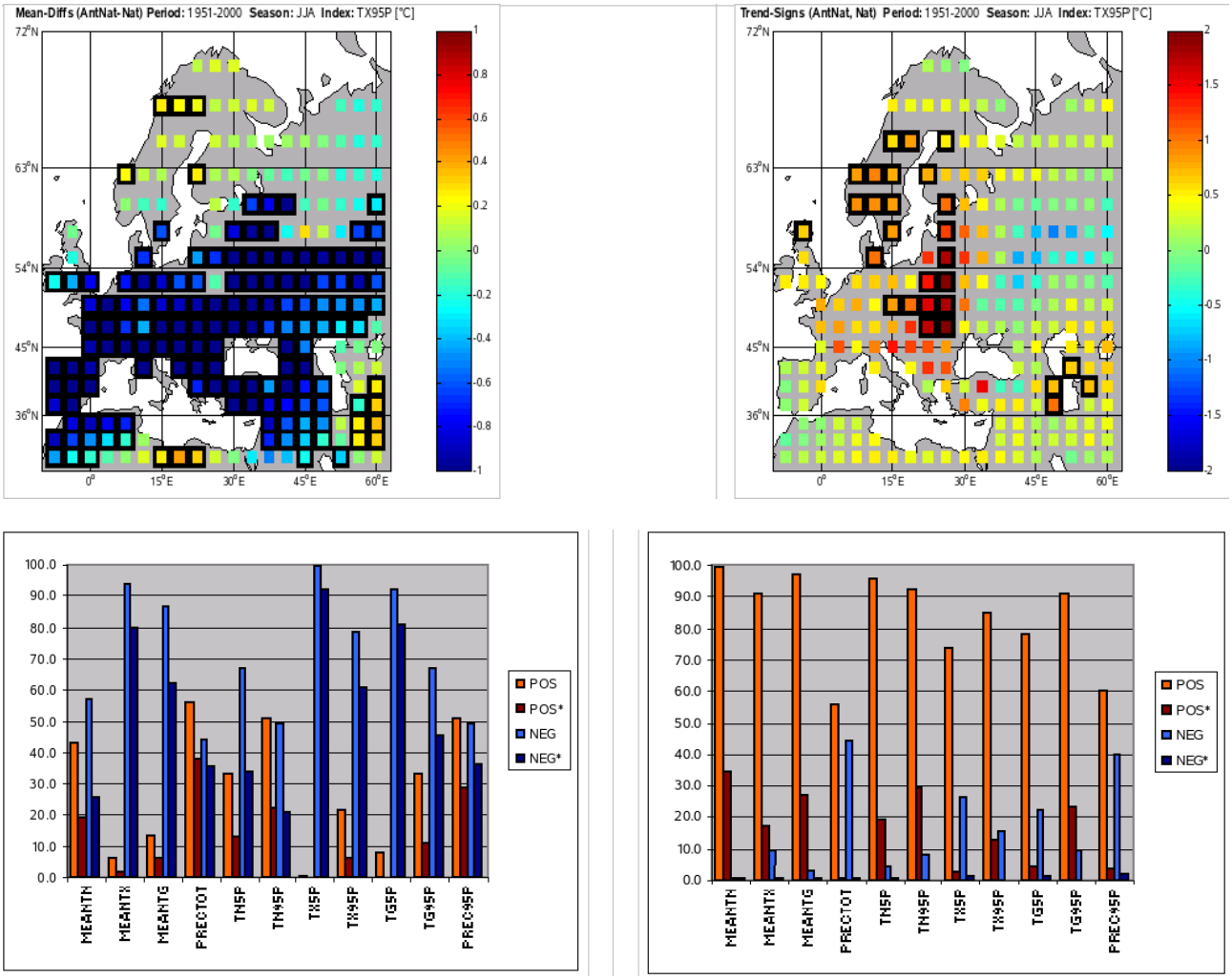

Fig. 4.9. Results for Europe showing differences between natural-plus-anthropogenic and natural-only forced ensemble simulations with HadAM3 for the period 1951-2000. The maps show differences in the ensemble means (left) and differences in ensemble-mean trends (right) for the TX95P index in the JJA season. Grid boxes with significantly (5% level) different means or trend slopes are marked with black boxes. The bar-diagram shows, for 11 different indices in the JJA season, the fraction [%] of grid-boxes where the differences in ensemble means (left) and differences in ensemble-mean trends (right) are positive and negative. POS: positive differences, POS*: positive significant differences (5% level), NEG: negative differences, NEG*: negative significant differences (5% level).

6.3.5 Work Package 5

The aim of this WP was to ensure that the project was effectively managed and datasets and deliverables made available over the project web site (see from cover of this report). The web site was set up in the first few months of the project and incorporated both external (to inform others about the project) and internal pages (for the use by the partners during the course of the project). At the end of the project all the Deliverables (either datasets or reports) are available from/via the web site. The majority are available directly from the web site, but D3 and the climate model integrations are available on the site of one of the partners. There are clear links from our main page to the available Deliverables. In addition, the datasets which have been created within the EMULATE Project are listed here in Table 6.1.

Dataset	Web location	Avail-ability
EMSLP daily pressure	http://www.hadobs.org/ (click in EMSLP)	Publicly available
Daily pressure (86 stns.)	http://www.cru.uea.ac.uk/projects/emulate/LANDSTATION_MSLP/	Publicly available
Daily temp/precip. series for 200+ stations	Not publicly available	Project only
Extreme climate/weather indices	http://www.cru.uea.ac.uk/projects/emulate/public/	Publicly available
Atmospheric circulation indices	http://www.cru.uea.ac.uk/projects/emulate/emslp3_pattern_classification/emslp3_pattern_classification/	Publicly available
scPDSI for Europe	http://www.cru.uea.ac.uk/projects/emulate/ (click on "A gridded database of drought ……."	Publicly available
HadAM3 output	http://www.hadc20c.org/ N.B. it is necessary to enter into a licence agreement to obtain/use the data	Publicly available

Table 6.1: *The listing of datasets produced by the EMULATE Project*

The co-ordinator will maintain the site for at least the next three years, and the various parts of the final report will be posted on the site.

6.4 CONCLUSIONS INCLUDING SOCIO-ECONOMIC RELEVANCE, STRATEGIC ASPECTS AND POLICY IMPLICATIONS

The scientific achievements of EMULATE can be summarised as follows from Section 6.3:

- A gridded daily database of sea-level pressure (referred as EMSLP) has been developed for the period from 1850 for the region 25ºN to 70ºN; 70ºW to 50ºE on a 5º by 5º grid spacing).

- The dataset has been extensively compared with gridded sea level pressure produced by reanalyses, such as those developed by ECMWF (ERA-40).

- The daily pressure data have been clustered into circulation types for each traditional 3-month and all 2-month seasons. The most realistic method involves simulated annealing, where the number of cases in each cluster differ markedly between clusters. A number of the clusters with large numbers of cases, show patterns related to the NAO. Few of the pattern amplitude extremes reveal significant trends over the period since the 1860s.

- Studies of within-pattern variability indicate some tendencies on the decadal scale. This is indicative of climate variability being the result not only due to changes in the frequencies of the patterns, but also to within-pattern changes of the major circulation types.

- Overall, the variability of the circulation explained about 40-50% of the variability of an average European temperature series – more in winter, as expected, and less in summer.

- A cyclone tracking algorithm was used to investigate changes in storms tracks since 1881. A significant reduction of cyclone numbers is apparent in the central North Atlantic and the Mediterranean, associated with a northward movement of the North Atlantic storm track.

- The variability of the daily circulation was compared with SST patterns over the North Atlantic region. This showed that there was a strong influence of the North Atlantic Oscillation (NAO) in winter, which was reduced in summer (SNAO). More distant influences from the tropical Pacific (the El Niño/Southern Oscillation, ENSO, phenomenon) were evident over western Europe, but the response was markedly different between stronger and weaker positive phases of ENSO. There is thus a strong non-linearity in response.

- An ensemble of climate model integrations has been completed. The simulation using global historic SST fields involve two sets of forcing factors: natural forcings (solar and volcanic) only and combined anthropogenic (includes greenhouse gas and aerosol forcing) and natural factors. There were 6 ensemble members for the period 1869-2002 and 12 for the period 1949-2002 for both the natural and anthropogenic+natural forcing history.

- The daily circulation from the model simulations for the EMULATE region was classified into daily circulation types using the same algorithm as used for the observational database (EMSLP). The relationships between the circulation types and

surface temperature and precipitation patterns in the model were compared with those in the real world.

- The differences in surface temperature response across Europe in the model integrations suggest that sulphate aerosol forcing has played a relatively important role in not allowing European temperatures to warm as much as those for the global average.

- A gridded database for drought was developed for Europe (35°N - 70°N, 10°W – 60°E) with a spatial resolution of 0.5° x 0.5°) using the self-calibrating Palmer Drought Severity Index.

- A new approach to forecasting winter conditions in western Europe has been developed. This relates to the pattern of SST anomalies in the North Atlantic. A forecast for a cooler and drier winter was made in November 2005 and the December 2005 to March 2006 was markedly cooler and drier than normal. More work is required to assess the approach, but the benefits of successful seasonal forecasting are manifold.

- The model integrations have (and will) prove useful unravelling the importance of the natural and anthropogenic forcing factors and their effect on European temperature and precipitation patterns.

- An extensive database of daily maximum and minimum temperatures and precipitation totals has been developed.75 temperature and 121 precipitation series extend back to 1900.

- A new method for the homogenization of mean daily and extreme daily temperature measurements has been developed. The method can only be applied to regions of Europe where there is a high spatial density of sites, so was confined mainly to central Europe.

- Indices for 64 different measures of extremes were calculated for each of the series, although most analyses were based on a subset of 19. A trend atlas for these 19 indices has been developed for Europe for different periods of the 20th century.

- The series developed over Spain have been used to produce a new adjusted daily temperature database for the country for the period from 1850. The database was used to assess spatial and temporal variability and change. Three principal regions of Spain (the northern and western coasts, the Mediterranean coast and the central plain were shown to have different relationships with the major circulation anomalies affecting the Peninsula, the NAO and SOI.

- Linear trends over the period 1901-2000 show a warming for all European temperature indices investigated. There are, however, large regional differences in temperature trend patterns. Winter precipitation totals, north of 40°N, have increased significantly by ~12% per 100yr. Trends in 90^{th}, 95^{th} and 98^{th} percentiles of daily winter precipitation have been similar. There is an overall weak tendency for summer precipitation to have become slightly more intense but less common.

- Over the period 1880 to 2003, the length of summer heatwaves over western Europe has doubled and the frequency of hot days has increased by 173%. Western Europe's climate

has become more extreme than previously thought and the hypothesized increase in variance of future summer temperature has been a reality over the last 125 years.

- Around 46% of the variability in summer heat waves can be explained by a statistical model combining combination of summer SLP anomalies, summer Atlantic and Mediterranean SSTs and summer European precipitation anomalies as predictors. There seems to be some predictability of heat wave events and associated patterns of drought on the decadal scale.

- There are significant differences between the mean values and trends over 1951-2000 in the model simulations made with anthropogenic-plus-natural forcings compared to those made with natural-only forcings, both in temperature and precipitation extremes. Observed and model trends are much closer when the model integrations with anthropogenic forcing are used. Seasonal and regional patterns can be identified, but not all differences are statistically significant.

The principal results from EMULATE of use to stakeholders and other scientists are the databases currently on the project website. These include the gridded daily sea-level pressure database, the daily station series of temperature and precipitation and the derived indices. The daily station temperature and precipitation database has already been used by the FP6 ENSEMBLES project (http://www.ensembles-eu.org).

6.5 DISSEMINATION AND EXPLOITATION OF THE RESULTS

Various means of dissemination of the results of EMULATE have been used. The major focus for dissemination has been the project website (http://www.cru.uea.ac.uk/projects/emulate), which provides access to all project deliverables and to the various databases. The EMULATE website is especially important, so will be maintained (and the references updated when scientific papers appear) for at least three years after the end of the project.

EMULATE partners have written many peer-reviewed papers over the course of the project. A number have recently been submitted to journals and a number are planned to be completed just after the formal end date of the project (see Table 6.2). We also expect that other groups will become interested in writing more when the dataset availability becomes more widely known. This generally happens when the first papers appear in the scientific literature. EMULATE partners have also given many presentations at national, European and international meetings and conferences during the course of the project. The total number of conference-related publications runs to over 50 abstracts. In addition there have been several postgraduate theses.

In more detail, there are 34 refereed publications and 59 conference presentations (both oral and poster). Of those refereed, 17 are published, 8 are in press and 9 are in review. Of the conference presentations, 53 were oral and 6 were posters. The number of theses completed is 6 and there are 2 reports.

Experience with the EMULATE daily EMSLP product (Ansell *et al.,* 2006) has shown that, while useful for the diagnosis of temperature and precipitation extremes, it is not ideal for investigations of storminess because each daily field is a 24-hour mean. A new historical gridded *sub-daily* mean sea level pressure (MSLP) product will be needed, building on the EMSLP daily data set. A new data initiative being developed by the GCOS AOPC/OOPC Surface Pressure Working Group (SPWG) (http://www.cdc.noaa.gov/Pressure/), NOAA's ESRL and the Hadley Centre at the UK Met Office will produce a world-leading, state-of-the-art, historical gridded sub-daily MSLP data set over the Northern Hemisphere back into the mid-to-late 19th century. This will have greater ability to resolve individual storms and circulation variations, and could be used to explore a wide range of extremes and their changing patterns over time (e.g. storm intensity and frequency, storm surges). This data set will build on the daily EMULATE EMSLP compilation, and observations being collected and digitised in conjunction with the SPWG's International Surface Pressure Data Bank (ISPD) and the NOAA ESRL 20th Century Reanalysis Project to create a 100+ year reanalysis product using only sub-daily surface pressure data (Compo *et al.,* 2006).

During our work on the North Atlantic Oscillation (NAO) for EMULATE, we investigated temperature and precipitation signals of the NAO over Europe. We discovered that there was statistically significant skill for forecasting both Central England and Northern European Temperature using our existing NAO forecasting method (developed under the EU FP5 PREDICATE project). We also discovered that this skill was higher than the skill of current dynamical model forecasts. We therefore extended our NAO forecast to provide a forecast temperature anomaly (http://www.metoffice.com/research/seasonal/regional/nao/index.html). The forecast NAO anomaly, and its demonstrated skill for temperature forecasts, was the

main piece of evidence in the Met Office headline winter forecast for 2005/6. The forecast predicted below average temperatures across Europe and generated widespread media interest. It has also lead to improved links between UK government contingency planners and the Met Office. A map of the actual temperature anomaly for the winter of 2005/6 showed good agreement with the forecast.

Finally, one interesting aside of the development of the daily gridded sea-level pressure dataset has been its usefulness for locating shipwrecks in the English Channel. The EMSLP data set for several days in early January 1852 was provided to Prof. Robin Pingree of the Plymouth Marine Laboratory (PML), who used these daily MSLP data to estimate ocean currents in the English Channel. This current information was used in their search for the likely position of a ship which sank on, or around, the 3rd - 4th of January in 1852 off Ushant, Brittany. As a result of their activities, and the use of the EMSLP derived current data, the previously lost wreck was located successfully. We have recently been involved in providing PML with EMSLP maps for further dates in January 1873 and May 1852. The Hadley Centre is looking to further collaborations of this type in other marine salvage actions.

6.6 MAIN LITERATURE PRODUCED

The EMULATE deliverables include a number of reports and information sheets (see Section 6.5 - above). These are supported by scientific papers in peer-reviewed journals. For a full listing of all peer-reviewed material that has been published or is within the peer-review system, see Section 2 of the Final Report. The total number of refereed publications is currently 34. Of these, 17 have been published, 8 are "in press" and a further 9 are "submitted". Several more are still in preparation, and these include:

Authors	Date	Title/subject
Brunet, M., Saladié, O., Jones, P.D., Sigró, J., Moberg, A., Aguilar, E., Walther, A., Lister, D. and López, D.	2006	The development of a new daily adjusted temperature dataset for Spain (1850-2003
Della-Marta, P. M., Haylock, M. R., Luterbacher, J. and Wanner H.	2006	The length of western European summer heatwaves has doubled since 1880.
Fereday, D.R., Knight, J.R., Scaife, A.A., Folland, C.K. and Phillipp, A.	2006	Cluster analysis of North Atlantic/European weather types.

Table 6.2: *Additional peer-reviewed publications that are in preparation.*

REFERENCES

Ansell,T.J., P.D. Jones, R.J. Allan, D. Lister, D.E. Parker, M. Brunet, A. Moberg, J. Jacobeit, P. Brohan, N.A. Rayner, E. Aguilar, M. Barriendos, T. Brandsma, N.J. Cox, P.M. Della-Marta, A. Drebs, D. Founda, F. Gerstengarbe, K. Hickey, T. Jónsson, J. Luterbacher, Ø. Nordli, H. Oesterle, M. Petrakis, A. Philipp, M.J. Rodwell, O. Saladié, J. Sigro, V. Slonosky, L. Srnec, V., 2006: Daily mean sea level pressure reconstructions for the European-North Atlantic region for the period 1850-2003. *J. Climate* (in press).

Basnett, T. and Parker, D. E., 1997: Development of the Global Mean Sea Level Pressure Data Set GMSLP2, *CRTN* 79, Hadley Centre, Met Office, Exeter, UK,16pp.

Beck, C., J. Jacobeit & P.D. Jones, 2006: Frequency and within-type variations of large-scale circulation types and their effects on low-frequency climatic variability in Central Europe since 1780. Int. J. Climatol. (conditionally accepted).

Bhend, J., 2005: North Atlantic and European Cyclones: Their Variability and Change from 1881 to 2003. Master's Thesis. Institute of Geography, University of Bern, Switzerland.

Brunet, M.., Saladié, O., Jones, P. D., Sigró, J., Moberg, A., Aguilar, E., Walther, A., Lister, D., Y López, D., 2006: The development of a new daily adjusted temperature dataset for Spain (1850-2003, *International Journal of Climatology* (in press).

Chapman, S. and Lindzen, R. S., 1970: *Atmospheric Tides*. D. Reidel, 200 pp.

Chen, D. and Walthe,r A., 2006: Preliminary results of attempts to detect an anthropogenic influence on extreme and mean climate and trends using the HadAM3 GCM. Manuscript, contribution to EMULATE D16, available on the project website.

Chen, D., Walther, A., Moberg, A., Jones, P. D., Jacobeit, J., Lister, D., 2006: Trend atlas of the EMULATE indices: Extreme temperature and precipitation climates over Europe. Göteborg University, Earth Sciences Centre, Report C73. ISSN 1400-383X, Göteborg, XX pp.

Compo, G.,P., Whitaker, J.,S. and Sardeshmukh, P.,D., 2006: Feasibility of a 100-year reanalysis using only surface pressure data, *Bulletin of the American Meteorological Society*, **87**, 175-190.

Dai, A. and Wang, J., 1999: Diurnal and semidiurnal tides in global surface pressure fields, *J. Atmos. Sci.*, **56**, 3874-3891.

Della-Marta, P., 2006: North Atlantic and European winter Cyclone Changes from 1881-2003. EMULATE manuscript, available via the EMULATE website (see complementary components for WP2).

Della-Marta, P. M., Wanner, H., 2006: A method of homogenizing the extremes and mean of daily temperature measurements. *J Climate* (in press).

Della-Marta, P. M., Haylock, M. R., Luterbacher, J. and Wanner H., 2006a: The length of western European summer heatwaves has doubled since 1880. (manuscript in preparation).

Della-Marta. P. M., Luterbacher, J., von Weissenfluh,. H., Xoplaki,. E., Brunet, M. and Wanner, H. 2006b: Summer heat waves over western Europe 1880-2003, their change and relationships to large scale forcings. *Climate Dynamics* (in review).

Diaz, H., Folland, C.K., Manabe, T., Parker, D.E., Reynolds, R., Woodruff, S., 2002: Workshop on Advances in the Use of Historical Marine Climate Data. *CLIVAR exchanges*, **25**, 71-73.

Fereday, D.R., Knight, J.R., Scaife, A.A., Folland, C.K. and Phillipp, A., 2006: Cluster analysis of North Atlantic/European weather types. (to be submitted).

Folland, C.K., Owen, J., Ward, M.N. and Colman, A.W., 1991: Prediction of seasonal rainfall in the Sahel region using empirical and dynamical methods. *J. Forecasting,* **10,** 21-56.

Folland, C.K., Parker, D.E., Ward, M.N. and Colman, A.W., 1988: Sahel rainfall, Northern Hemisphere circulation anomalies and worldwide sea temperature changes. *Proc. study week, 'Persistent meteo-oceanographic anomalies and teleconnections', Pontifical Academy, Rome, 23-27 Sept 1986.* Eds. C.Chagas and G.Puppi, pp 393-436, Pontificia Academia Scientiarum Scripta Varia **69**.

Gordon, C., Cooper, C., Senior, C.A., Banks, H., Gregory, J.M., Johns, T.C., Mitchell, J.F.B. and Wood, R.A., 2000: The simulation of SST, sea ice extents and ocean heat transports in a version of the Hadley Centre coupled model without flux adjustments. *Climate Dynamics,* **16,** 147-168.

Hartigan, J. A. and M. A. Wong, 1979: A K-Means Clustering Algorithm. *Applied Statistics* **28**, 100-108.

Jackson, M., 1986: Operational Superfiles, *Met O 13 Technical Note* 25.

Jacobeit, J., 1993: Regionale Unterschiede im atmosphärischen Zirkulationsgeschehen bei globalen Klimaveränderungen. *Die Erde* **124(1)**, 63-77.

Jacobeit, J. et al., 2003: Atmospheric circulation variability in the North-Atlantic-European area since the mid-seventeenth century. *Clim Dyn* **20**, 341-352.

Jacobeit, J., Rathmann, J. and Philipp, A., 2006a: Trend matrices for regional climatic time series. Manuscript, contribution to D14, available on the project website.

Jacobeit, J., Rathmann, J. and Philipp, A., 2006b: Daily MSLP classifications and PCA-derived circulation patterns in relation to temperature and precipitation extremes. Manuscript, contribution to D15, available on the project website.

Jacobeit, J., A. Philipp & M. Nonnenmacher, 2006c: Atmospheric circulation dynamics linked with prominent discharge events in Central Europe (submitted).

Jones, P. D. et al, 1999: Monthly mean pressure reconstructions for Europe for the 1780-1995 period, *Int. J. Climatol*., **19**: 347-364.

Kalnay, E. et al., 1996: The NCEP/NCAR 40-year reanalysis project, *Bulletin of the American Met Societ*y, **77**, 437-471.

Kaplan, A., Kushnir, Y., Cane, M. A., 2000: Reduced space optimal interpolation of historical marine sea level pressure: 1854-1992, *J. Climate*, **13**, 2987-3002.

Knight, J. R., Allan, R. J., Folland, C. K., Vellinga, M. and Mann, M.E., 2005: A signature of persistent natural thermohaline circulation cycles in observed climate, *Geophysical Research Letters,* **32,** L20708, doi:10.1029/2005GL024233.

Linderholm, H.W., 2006: Reconstructing summer NAO back to 1706 with tree-ring data. EMULATE manuscript, available via the EMULATE website (see complementary components for WP2).

Linderholm, H. W., Walther, A. and Chen, D., 2005: Growing season trends in the greater Baltic area. Göteborg University, Earth Sciences Centre, Report C69, ISSN 1400-383X, Göteborg, 88 pp.

Lukashin, A. V. & R. Fuchs, 2001: Analysis of temporal gene expression profiles: clustering by simulated annealing and determining the optimal number of clusters. Bioinformatics 17: 405-414.

Moberg, A., Jones, P.D., Lister, D., Walther, A., Brunet, M., Jacobeit, J., Alexander, L. V., Della-Marta, P. M., Luterbacher, J., Yiou, P., Chen, D., Klein Tank, A. M. G., Saladié, O., Sigró, J., Aguilar, E,, Alexandersson, H., Almarza, C., Auer, I., Barriendos, M., Begert, M., Bergström, H., Böhm, R., Butler, J. C., Caesar, J,, Drebs, A., Founda, D., Gersengarbe, F-W., Micela, G., Maugeri, M., Österle, H., Pandzic, K., Petrakis, M., Srnec, L., Tolasz, R., Tuomenvirta, H., Werner, P. C., Linderholm, H., Philipp, A., Wanner, H. and Xoplaki, E.. 2006: Indices for daily temperature and precipitation extremes analysed for the period 1901-2000. *Journal of Geophysical Research – Atmospheres* (in review).

Monahan, A.H., 2001: Nonlinear principal component analysis: tropical Indo-Pacific sea surface temperature and sea level pressure. J Climate 14: 219-233.

Murray, R. & Simmonds, I., 1991: A numerical scheme for tracking cyclone centres from digital data, Part I: development and operation of the scheme. Australian Meteorological Magazine 39: 155-166.

Mohammad, R., Moberg, A, and Ansell, T., 2006: Correlations between indices for temperature and precipitation extremes in Europe and the leading atmospheric circulation mode during 1901-2000. Manuscript, contribution to D11 and D15, available on the project website.

Parker, D. E., 1984: The statistical effects of incomplete sampling of coherent data series, *J. Climatol*., **4**, 445-449.

Philipp, A., Della-Marta, P. M., Jacobeit, J., Fereday, D. R., Jones, P. D., Moberg, A.and Wanner, H., 2006: Long-term variability of daily North Atlantic-European pressure patterns since 1850 classified by simulated annealing clustering. *Journal of Climate* (submitted).

Philipp, A., J. Jacobeit & P.M. Della-Marta, 2005: Classifying reconstructed daily pressure patterns for the period 1850 to 2003 in the North-Atlantic-European Region by Simulated Annealing Clustering. – In: Proceedings of COST733 Meeting Utrecht, EMS 5th Annual Meeting 2005, (in press).

Rayner, N.A., Parker, D.E., Horton, E.B., Folland, C.K., Alexander, L.V, Rowell, D.P., Kent, E.C. and Kaplan, A., 2003: Global analyses of sea surface temperature, sea ice and night marine air temperature since the late nineteenth century. *J. Geophys. Research (Atmospheres),* **108** (D14), 4407, 10.1029/2002JD002670 (29 pp. + 8 supplementary colour pages).

Reynolds, R. W., 1988: A real-time global sea surface temperature analysis, *J. Climate*, **1**, 75-86.

Rodwell, M.R. and Folland, C.K., 2002: Atlantic air-sea interaction and seasonal predictability. *Quarterly J. Royal Meteorological Soc.,* **128**(583), 1413-1443.

Scaife, A., Knight, J. R., Vallis, G. K. and Folland, C.K., 2005: A stratospheric influence on the winter NAO and North Atlantic, *Geophysical Research Letters,* **32,** L18715, doi:10.1029/2005GL023226.

Sexton D. M. H., Grubb, H., Shine, K.P. and Folland, C.K., 2003: Design and analysis of climate model experiments for the efficient estimation of anthropogenic signals, *J. Climate*, **16**, 1320-1336.

Shapiro, R., 1971: The use of linear filtering as a parameterization of atmospheric diffusion, *J. Atmos. Sci.*, **28**, 523-531.

Smith, D.M., Cusack, S., Colman, A.W., Folland, C.K. and Murphy, J.M., 2006: Improved surface temperature prediction for the coming decade from a global climate model. Submitted to *Nature.*

Stephenson, D. B., A. Hannach & A. O'Neill, 2004: On the existence of multiple climate regimes. *Q. J. Roy. Met. Soc.* **130,** 583-606.

van der Schrier, G., Briffa, K.G., Jones, P. D. And Osborn, T.J., 2006: Summer moisture availability across Europe, *Journal of Climate* (in press).

Yiou, P. and Fauchereau, N., 2006: Surface temperature anomalies extremes and SLP cluster association. Manuscript, contribution to D15, available on the project website.